République **A**lgérienne **D**émocratique et **P**opulaire

Ministère de l'**E**nseignement **S**upérieur et de la **R**echerche **S**cientifique

Université 20 août 1955-Skikda

Faculté des Sciences

Département de Physique

N° : DP202302MM

Mémoire de Master

Filière : Physique

Spécialité : Matériaux

Thème

Synthesis and characterization of ZnS thin films deposited by ultrasonic spray technique

---

Présenté par :

NAILI Khouloud

Soutenu le 03/07/2023 devant le jury composé de :

A.FEKRACHE	MCA	Université de Skikda	Président
K. KAMLI	MCA	Université de Skikda	Rapporteur
Z.HADEF	MCA	Université de Skikda	Examinateur

Année Universitaire : 2022/2023

Abstract

The present work deals with the deposition and characterization of ZnS thin films. Our main goal is the synthesis and characterization of those thin films which were deposited by ultrasonic spray technique, and applicate them in the field of solar cells. In the first and second part we have studied the ZnS properties and applications, the diposition technique and the basics of the solar cells. In the second part ZnS thin films were deposited on glass substrates heated at 300°C, 400°C and 500°C, those elaborated films were characterized in order to study their properties using different characterization methodes such as : XRD, SEM, EDS and Spectrophotometry.

Keywords : ZnS, thin films, spray pyrolysis, solar cells, substrat temperature, characterization.

Resumé

Le présent travail porte sur le dépôt et la caractérisation de couches minces de ZnS. Notre objectif principal est la synthèse et la caractérisation de ces couches minces qui ont été déposés par la technique de spray ultrasonique, et de les appliquer dans le domaine des cellules solaires. Dans la première et la deuxième partie, nous avons étudié les propriétés et les applications du ZnS, la technique de déposition et les bases des cellules solaires. Dans la deuxième partie, des films minces de ZnS ont été déposés sur des substrats de verre chauffés à 300°C, 400°C et 500°C, ces films élaborés ont été caractérisés afin d'étudier leurs propriétés en utilisant différentes méthodes de caractérisation telles que : DRX, MEB, EDS, Spectrophotométrie.

Mots-clés : ZnS, couches minces, spray ultrasonique, cellules solaires, température de substrat, caractérisation.

ملخص

هذا العمل يهتم بترسيب وتشخيص الشرائح الرقيقة لZnS . هدفنا الرئيسي هو تركيب وتوصيف تلك الأغشية الرقيقة التي ترسبت بتقنية الرش(الانحلال الحراري)، وتطبيقها في مجال الخلايا الشمسية. درسنا في الجزء الأول والثاني خصائص وتطبيقات ZnS، وتقنية الترسيب وأساسيات الخلايا الشمسية. في الجزء الثاني، تم ترسيب أغشية ZnS الرقيقة على ركائز زجاجية مسخنة عند 300 درجة مئوية و 400 درجة مئوية و 500 درجة مئوية وتم تشخيص تلك الشرائح الرقيقة لدراسة خصائصها باستخدام طرق معالجة مختلفة مثل: XRD و SEM و EDS و قياس الطيف الضوئي.

الكلمات المفتاحية: ZnS، الشرائح الرقيقة، الانحلال الحراري بالرش، الخلايا الشمسية، درجة الحرارة، التشخيص.

Acknowledgements

In the name of Allah, the Most Gracious and the Most Merciful

Alhamdullilah, all praise to Allah for all His blessing in the completion of this thesis.

First and foremost, I would like to express my deep and sincere gratitude to my supervisor, *Prof KAMLI KENZA* for her guidance and help.

Words are lacking to express thanks to my loving parents, my first school ever as my road to this stage is the result of their efforts, prayers, inspiring response and encouragement throughout my life.

Finally, I won't forget anyone who helped me with this work even if with just a word of encouragement.

Dedication

In the name of **Allah**, the most merciful and the most gracious.

To the most precious two in my life, who gave me everything, who

builtme up to who I am today, words will never e enough to express my gratitude , may allah keep you a blessing in my life for the longest time, My **dear father** and my **wonderful mother** may allah bless you.

To my precious **family,** everyone by their name, who I found by my side everytime I needed.

To my second family, who we shared the laughs and the cries, my **dear friends**. Especially **Hana** and **Manel**, may Allah bless them.

To my besty who stucked with me through thick and thin especially this year: **Bouchra.**

To Amira who worry about my studies and future more than me.

To every passenger in my life, to anyone who left a trace in my heart, to the words didn't mention but my heart never forget, to ones who was close someday but we will not cross paths again and finally the ones who left us early, the ones in the graves but never left the heart.

Khouloud.

Index

Index

Chapter II : Solar cells technology

Index

Practical part

Chapter III : ZnS elaboration

Chapter IV : Results and discussion

List of figures

List of figures

Liste of tables

General Introduction

The field of thin films is an old but very important project, it passed to numerous modifications and led to a major research effort which was undertaken in recent years in several technological fields to meet a set growing needs [1].

Recently, the II-VI compounds semiconductor thin films (e.g CdS, ZnS, Cdse, ZnSe …) have received an intensive attention due to their application in thin film solar cell, optical coatings, optoelectronic devices and light emitting diodes [2]. Among these metals, a Chalcogenides ZnS is an important semiconductor material, his wide direct band gap and n-type conductivity are promising for optoelectronic device applications, such as electroluminescent devices and photovoltaic cells. In optoelectronics, it can be used as light emitting diode in the blue to ultraviolet spectral region due to its wide band gap of 3.7 eV at room temperature. In the area of optics, ZnS can be used as a reflector and dielectric filter because of its high refractive index (2.35) and high transmittance in the visible range, respectively.

In recent times, the study of semiconductors in the bulk has been replaced with that of thin films. Thin film technique is one of the most fully-fledged technologies that greatly contribute to developing the study of semiconductors by giving a clear indication of their chemical and physical properties. Thin films have mechanical, electrical, magnetic and optical properties which may differ from those of the bulk material and are used commonly in the form of a deposit on a suitable substrate. Presently, rapidly changing needs for thin film materials and devices are creating new opportunities for the development of new processes, materials and technologies.

There exists a huge variety of thin film deposition processes and technologies which originate from purely physical or purely chemical processes. These include vacuum evaporation, spray pyrolysis, sputtering molecular beam epitaxy, vapour phase epitaxy, chemical vapour deposition, solution growth, screen printing and electrophoresis. Despite the existence of these large variety of deposition techniques, searching for the most reliable and economic deposition technique has always been the main goal [3]. The spray pyrolysis technique has several advantages including the higher stability of the obtained coatings as compared to coatings deposited in vacuum, the diversity of its solution precursors, its cost-effectivity, and its facility [4].

Oil and gas, which are at present the source of energy, will eventually be exhausted after sometime. This necessitates the search for renewable energy source. Sun is a high source of energy that can be converted into electrical energy using the solar cell which is the best non-pollutant alternative energy source. Because of increasing demand for energy and the limited supply of fossil fuels, the search for alternative source of power is imperative. Given that there is a vast amount of energy available from the sun, and devices that convert light energy into electrical energy are becoming important. A solar or photovoltaic cell converts light energy into electrical power [2].

Different of the semiconductor materials with suitable optoelectronic properties have been found for photovoltaic applications. Silicon is the most commonly used active material for solar cells applications, with over the 85 % of the whole photovoltaic market dominated by crystalline silicon wafer technology. monocrystalline and polycrystalline silicon based solar cells have efficiencies approaching 20 - 25 %. However, despite new technologies that reduce the use of silicon exist, alternative materials and solutions are studied. This has led the photovoltaic industry to produce thin film solar cells consisting of cheaper materials and smaller thickness. The efficiencies reached by the thin film solar cells result lower than silicon wafer cells, being of about 10 – 15 %. However, the ratio of efficiency to price makes these cells competitive in the photovoltaic market, with wider possibilities to improve the efficiency . Thin film solar cells are made by deposition of more thin layers on a rigid substrate, with the presence of passivating material layers in the front and rear surfaces to reduce the surface recombination of minority carriers, which is among the major causes of efficiency loss [5].

In this thesis, a characterization of a series of ZnS thin layers has been performed with diffrent techniques such as XRD, SEM, EDS… to evaluate the main features. ZnS thin films deposited on a substrate by Ultrasonic Spray pyrolysis at have been studied in the analysis. And a simulation using the software SCAPS was done with the results of the analysis.

The present manuscript has been divided into four chapters. The first chapters is dedicated to present a bibliographic study providing a general look around thin films and its deposition and characterization methods, as well as a full explanation of spray pyrolysis technique, therefore, mention of some optical, electrical and structural properties of the ZnS.

The second chapter is dedicated to present the principes of solar cells such as the photovoltaic effect, it’s characteristics and figures of merit, as well as the diffrent reasons in those cells.

The third chapter dedicated to highlighting all the operating methods and used materials during the whole study. Finally, we finish this manuscript with collecting and discussing all the results obtained along this study.

References

[1] B. Rafia, *Caractérisation Spectroscopique des Couches minces d'oxyde de Nikel (NiO) Elaborées par Spray, doctorate thesis, Université Kasdi Merbah Ouargla,* 2018.

[2] Odunaike R.K, Akande Ademola, «Synthesis of Zinc Sulfide (Zns) Thin Films by Chemical Deposition Technique and its Optical Characterization,» *International Journal of Trend in Research and Development,* vol. 5, n° %11, pp. 288-298, 2021.

[3] A. O. ANSAH, *INVESTIGATING THE OPTICAL PROPERTIES OF ZINC SULPHIDE THIN FILMS DEPOSITED FROM CHEMICAL ACIDIC BATHS, master thesis,* 2012.

[4] Saeed Rahemi Ardekani, Alireza Sabour Rouh Aghdam, Mojtaba Nazari, Amir Bayat, Elnaz Yazdani, Esmaiel Saievar-Iranizad, «A comprehensive review on ultrasonic spray pyrolysis technique: Mechanism, main parameters and applications in condensed matter,» *Journal of Analytical and Applied Pyrolysis,* vol. 141, 2019.

[5] A. Bartolucci, *Morphological characterization of ZnS thin films for photovoltaic applications,* 2015.

Theoretical part

Chapter I : Bibliographic synthesis

I.1. Introduction

Production, application and research of thin films date back a rather long time. Nowadays, thin films are widespreadly applied as functional coatings that advantageously influence the properties of the substrate device due to the films's certain surface characteristics. Number of thin film deposition techniques have been developed in the last century, parallely with the improvement of electronics, vacuum- and measurement technologies [1], This technology is still undergoing rapid changes which will lead to even more complex and advanced electronic devices in the future [2].

This chapter covers the fundamentals of the thin film technology, including deposition and characterization techniques and the different properties of zinc sulfide such as structural, optical and electrical properties. Due to the exceptional diversity of thin films and the large range of applications it is complicated to cover in detail all the areas.

I.2. Thin films : an overview

I.2.1. Definition of a thin film (layer)

It is possible to define a thin film of a material that is an element of this material so that its thickness is greatly reduced, which is expressed with nanometers. (Layer quasi two dimensionality). The small distance between the two boundary surfaces gives a disturbance of the physical, chemical and mechanical properties [3].

The nature of thin layers can be insulating (SiO_2, SiN_4, SiC,), metallic (Al, Cr, Au, Ag, ...) and semi-conductor (Si, GaAs, CdTe, ZnO, ...). while its structure can be amorphous, nanocrystalline, microcrystalline or mono crystalline [4].

The essential difference between the material in the solid state and the state of thin layers is indeed related to the fact that in the solid state the role of the limits (the surfaces) is generally neglected with good reason in properties, whereas in a thin layer it is on the contrary the effects related to the boundary surfaces which are preponderant. It is obvious that the thinner the thickness, the more pronounced this two-dimensional effect will be, and conversely when the thickness of a thin layer exceeds a certain threshold the effect of thickness will become minimal and the material will regain the well-known properties of the solid material.

The second essential characteristic of a thin film is whatever the procedure used for its manufacture ; a thin film is always attached to a substrate on which it is built (even if, sometimes, it happens that one separates the thin film from the substrate). Consequently, it will be imperative to take this major fact into account in the design, namely that the support strongly

influences the structural properties of the layer deposited there. Thus, a thin layer of the same material, of the same thickness may have significantly different physical properties depending on whether it is deposited on an amorphous insulating substrate such as glass or a single-crystal silicon substrate for example.

The result of these two essential characteristics of a thin layer is that a thin layer is anisotropic by construction [5].

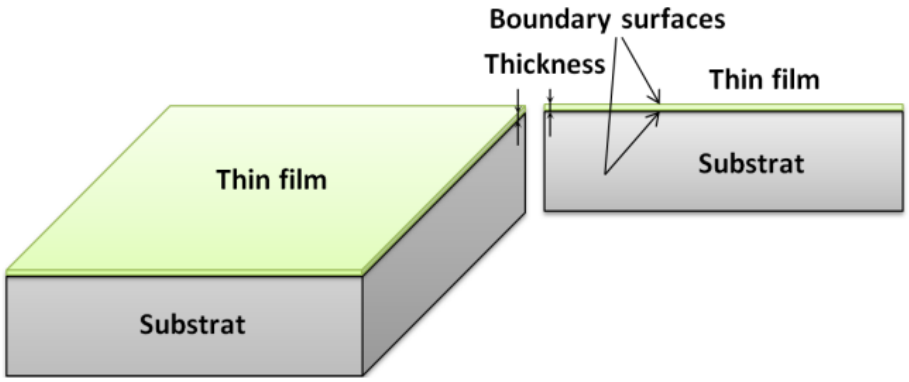

Figure I.1. Schematic of thin film deposited on a glass substrate [6]

I.2.2. Applications of thin films

Thin films offer enormous potential due to the following :

- ✓ Conservation of scarce materials.
- ✓ Production of nanostructured coatings and nanocomposites.
- ✓ Ecological considerations—a reduction of effluent output and power consumption.
- ✓ Improved functionality of existing products.
- ✓ Solution to previously unsolved engineering problems.
- ✓ Creation of entirely new and revolutionary products [7].

That results the usage of thin films in modern technology for different applications. Thin film materials have already been used in semiconductor devices, wireless communications, telecommunications, integrated circuits, rectifiers, transistors, solar cells, light-emitting diodes, photoconductors, light crystal displays, magneto-optic memories, audio and video systems, compact discs, electro-optic coatings, memories, multilayer capacitors, flat-panel displays, smart windows, computer chips, magneto-optic discs, lithography, microelectromechanical systems (MEMS), and multifunctional emerging coatings, as well as other emerging cutting technologies [8].

I.3. Thin-Film Deposition Processes and Technologies

I.3.1. The importance of deposition Technology in modern fabrication processes

The technology of thin film deposition has advanced dramatically during the past 30 years.This advancement was driven primarily by the need for new products and devices in the electronics and optical industries,where deposition technology can well be regarded as the major key to the creation of devices such as computers, since microelectronic solid-state devices are all based on material structures created by thin-film deposition. Electronic engineers have continuously demanded films of improved quality and sophistication for solid-state devices, requiring a rapid evolution of deposition technology. Equipment manufacturers have made successful efforts to meet the requirements for improved and more economical deposition systems and for in situ process monitors and controls for measuring film parameters. Another important reason for the rapid growth of deposition technology is the improved understanding of the physics and chemistry of films, surfaces, interfaces, and microstructures made possible by the remarkable advances in analytical instrumentation [2].

I.3.2. Classification of deposition technologies

Thin-films are in general developed to provide special properties, i.e. electrical, optical, mechanical, chemical, that satisfy the needs for specific applications. The desired properties are determined by the resulting film structure, which strongly dependents on the selected deposition method, film material, and substrate. In line with the wide range of applications of thin films, a number of deposition methods have been developed/improved to optimize the film properties [9], and The aim of any deposition technique is the preparation of thin films in reproducible, controllable and predictive ways [10].

Since the concern here is with thin-film deposition methods for forming layers in the thickness range of a few nanometers to about ten micrometers, the task of classifying the technologies is made simpler by limiting the number of technologies to be considered.

Basically, thin-film deposition technologies are either purely physical, such as evaporative methods, or purely chemical, such as gas- and liquid-phase chemical processes. A considerable number of processes that are based on glow discharges and reactive sputtering combine both physical and chemical reactions ; these overlapping processes can be categorized as physical-chemical methods [2].

A. Physical deposition methods (PVD)

Physical deposition methods are usually referred as to physical vapor deposition methods (PVD) because the process entails the generation of vapor. PVD essentially consists in removing growth species from a source or target material via evaporation, then this vapor is

transported to the substrate surface, and eventually it solidifies in the surface, forming the film [9].

B. Chemical deposition methods (CVD)

CVD is a deposition method where a volatile compound of a pre-established substance is introduced into a reactor, usually along with an inert gas, to induce a chemical reaction which produces a solid thin film onto a substrate [9] which often require high temperature and therefore limit the choice of substrate material [11].

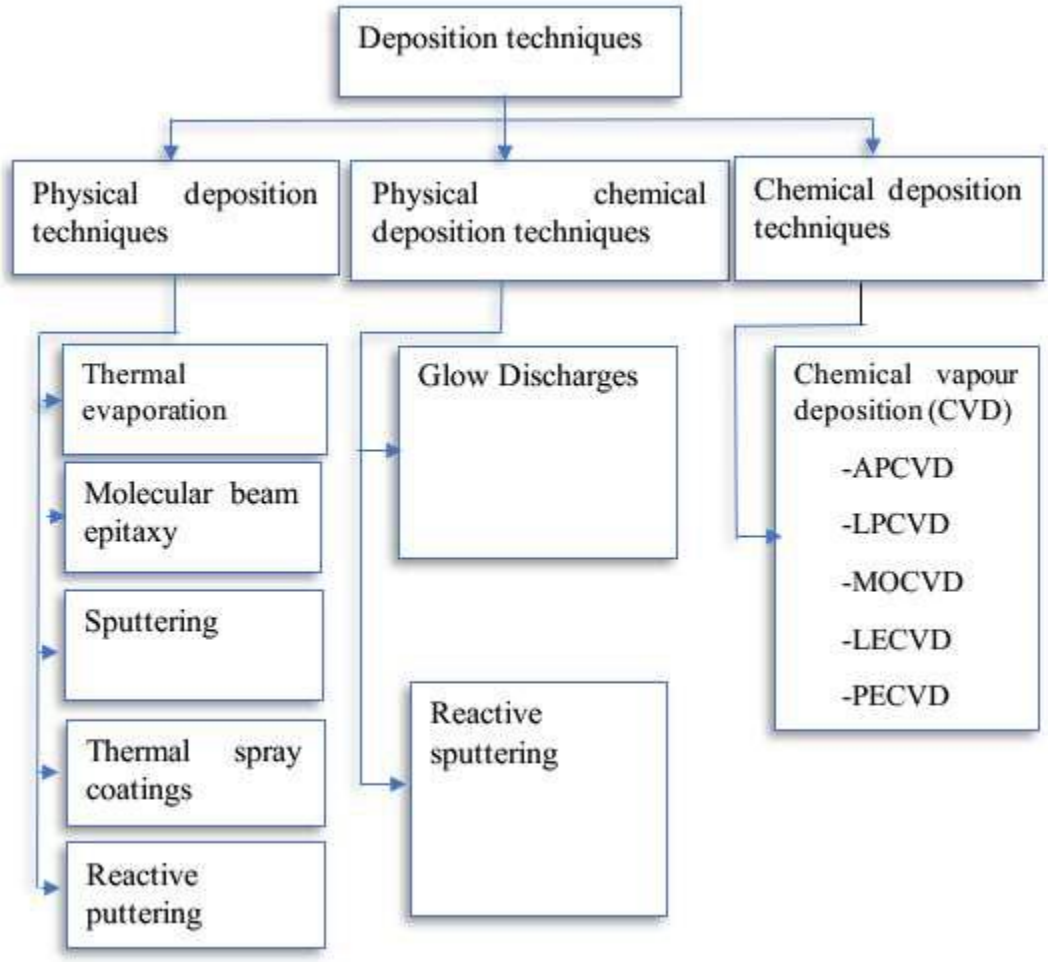

Figure I.2. Survey and Classification of Thin-Film deposition Technologies [2]

Another classification scheme is presented in **Table I.1** where we have grouped thin-film deposition technologies according to evaporative glowdischarge, gas-phase chemical, and liquid-phase chemical processes.

Table I.1. Classification of Thin-Film Depositon Technologies [2]

Evaporative Methods	
• Vacuum Evaporation	
Conventional vacuum evaporation	Molecular-beam epitaxy (MBE)
Electron-beam evaporation	Reactive evaporation
Glow-Discharge processes	
• Sputtering	**• Plasma Processes**
Diode sputtering Reactive sputtering Bias sputtering (ion plating) Magnetron sputtering Ion beam deposition Ion beam sputter deposition Reactive ion plating Cluster beam deposition (CBD)	Plasma-enhanced CVD Plasma oxidation Plasma anodization Plasma polymerization Plasma nitridation Plasma reduction Microwave ECR plasma CVD Cathodic arc deposition
GAS-PHASE CHEMICAL PROCESSES	
• Chemical Vapor Deposition (CVD)	**• Thermal Forming Processes**
CVD epitaxy Atmospheric-pressure CVD (APCVD) Low-pressure CVD (LPCVD) Metalorgainc CVD (MOCVD) Photo-enhanced CVD (PHCVD) Laser-induced CVD (PCVD) Electron-enhanced CVD	Thermal oxidation Thermal nitridation Thermal polymerization Ion implantation
LIQUID-PHASE CHEMICAL TECHNIQUES	
• Electro Processes	**• Mechanical Techniques**
Electroplating Electroless plating Electrolytic anodization Chemical reduction plating Chemical displacement plating Electrophoretic deposition	Spray pyrolysis Spray-on techniques Spin-on techniques Liquid phase epitaxy

I.3.3. Deposition Steps of thin films

All thin film deposition processes contain four steps successive, as shown in **Figure I.3**.

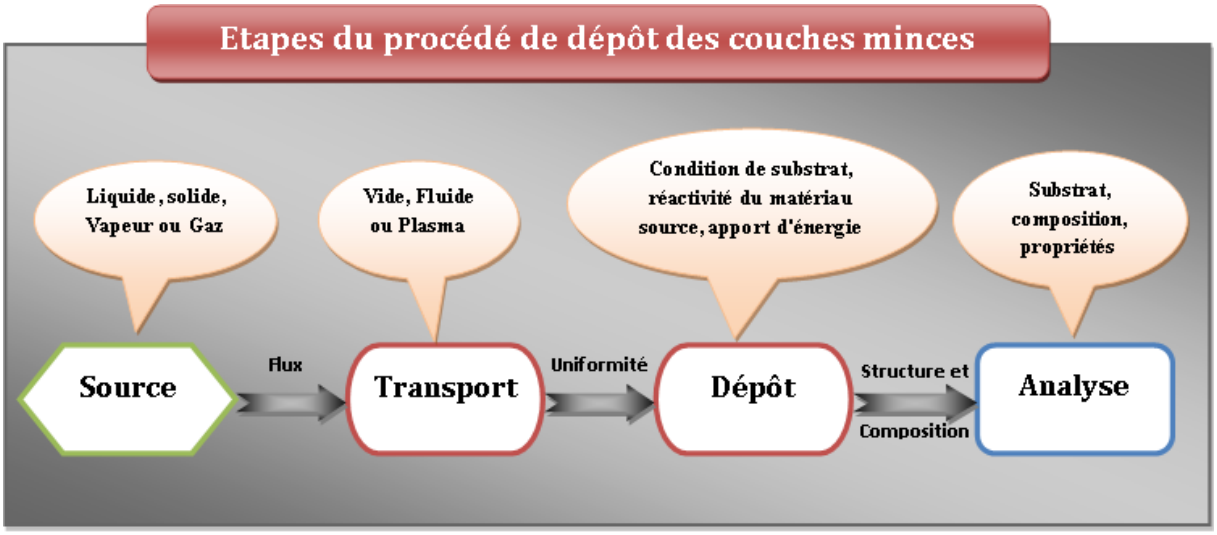

Figure I.3. Diagram of the stages of the thin film deposition process [3]

I.4. Ultrasonic Spray pyrolysis

I.4.1. General Description of Spray pyrolysis

The spray pyrolysis technique is an adaptable processing method for preparing single- and multi-layered films as dense or porous, ceramic coatings, and various material powders [12]. Unlike many other film deposition techniques, spray pyrolysis represents a very simple and relatively cost-effective processing method, It offers an extremely easy technique for preparing films of any composition. Spray pyrolysis does not require high-quality substrates or chemicals [10].

The existing spray processing techniques can be classified either based on the type of the energy source for the starting solution reaction for the spray pyrolysis process including tubular reactors (SP), the emulsion combustion method, vapor flame reactors, and the flame spray pyrolysis, or based on the method used for atomizing precursors, including electrostatic, air-pressurized, and ultrasonic spray pyrolysis techniques. Another classification of spray pyrolysis techniques is based on the type of atomizers employed in the system. Furthermore, the aerosol droplet size, which specifies the obtained film quality, depends commonly on the atomization method. There are three main atomization methods: electrostatic, air blast, and ultrasonic [13].

A typical spray pyrolysis system is composed of a reservoir for precursor solution, droplet generator, reactor, and collection unit as shown in **Figure I.4**. Precursor solutions of aqueous or nonaqueous solvents are atomized and carried by a gas into a reactor in which droplets are evaporated and decomposed into solid particles. Nucleation and growth of monomer precursor are also involved in the process of particle formation. Electrical heating or flame provides heat for evaporation of solvent and decomposition of precursor. Some nonconventional heating methods such as microwave or laser are employed for controlling morphology [14].

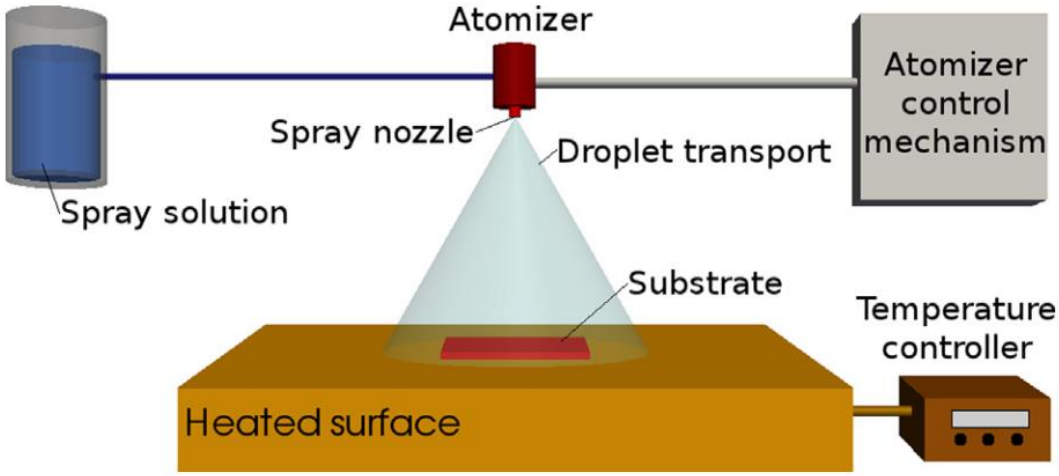

Figure I.4. General schematic of a spray pyrolysis deposition process [14]

The basic principle of this technique is that, when droplets of the spraying solution gets in contact with the hot substrate, due to the pyrolytic decomposition of solution and the free pin-hole, the film is deposited uniformly on the substrates [15].

I.4.2. Spray pyrolysis advantages

Spray pyrolysis technique is advantageous in a variety of ways when compared to other technique, amongst which includes:

- ✓ Unlike closed vapour deposition methods, SP does not require high quality targets and/or substrates nor does it require vacuum at any stage, which is a great advantage if the technique is to be scaled up for industrial applications.
- ✓ The deposition rate and the thickness of the films can be easily controlled over a wide range by changing the spray parameters, thus eliminating the major drawbacks of chemical methods such as sol–gel which produces films of limited thickness.

- ✓ It offers an extremely easy way to dope films with virtually any element in any proportion by merely adding it in some form to the spray solution.
- ✓ Operating at moderate temperatures (100–500°C), SP can produce films on less robust materials.
- ✓ Unlike high-power methods such as radio frequency magnetron sputtering (RFMS), it does not cause local overheating that can be detrimental for materials to be deposited. There are virtually no restrictions on substrate material, dimension or its surface profile.
- ✓ By changing composition of the spray solution during the spray process, it can be used to make layered films and films having composition gradients throughout the thickness.
- ✓ It is believed that reliable fundamental kinetic data are more likely to be obtained on particularly well characterized film surfaces, provided the films are quiet compact, uniform and that no side effects from the substrate occur. SP offers such an opportunity [16].

I.4.3. Processing steps of spray pyrolysis technique

Spray pyrolysis involves many processes occurring either simultaneously or sequentially. The most important of these steps are three processing steps that are presented and analyzed as follows:

1. Atomization of the precursor solution.
2. Aerosol transport of the droplet.
3. Decomposition of the precursor to initiate film growth [6].

These three steps are individually addressed in the sections to follow.

I.4.3.1. Precursor atomization

The atomization procedure is the first step in the spray pyrolysis deposition system. The idea is to generate droplets from a spray solution and send them, with some initial velocity, towards the substrate surface. Spray pyrolysis normally uses air blast, ultrasonic, or electrostatic techniques [14]. The atomizers differ in resulting droplet size, rate of atomization, and the initial velocity of the droplets. For electrical atomizers, it has been shown that the size of the generated droplet is not related to any fluid property of the precursor solution and depends solely on the fluid charge density level ρe as shown in equationI.1 :

$$r^2 = \left(\frac{-\alpha}{\beta}\right)\frac{3\varepsilon_0}{q\rho_e} \qquad \text{(I.1)}$$

Where ε_0 is the permittivity, q is the elementary charge, and 'α/β'is a constant value equal to ~1.0×10^{-17} J. The mass of a droplet, assuming a spherical shape depends on its density as shown in equation I.2:

$$m = \frac{4\pi}{3}\rho dr^3 \qquad \text{(I.2)}$$

where r is the droplet radius. The initial leaving velocity of the droplet is an important parameter as it determines the rate at which the droplets reach the substrate surface, the heating rate of the droplet, and the amount of time the droplet remains in transport the spray pyrolysis environment [8].Table I.2 summarizes the properties of droplets for different atomizers commonly used for spray pyrolysis deposition [17] :

Table I.2 Characteristics of atomizers commonly used for spray pyrolysis [17]

Atomizer	Droplet diameter (µm)	Droplet velocity (m/s)
Pressure	5 – 50	5 –20
Ultrasonic	1 –100	0.2-0.4
Electrostatic	5 –70	1–4

I.4.3.2. Aerosol transport of droplets

In an aerosol the droplet is transported and eventually evaporates. In case dense films are desired, it is important that during transportation as many droplets as possible fly to the substrate without forming particles before reaching the surface [18]. As the droplets move through the ambient, they experience physical and chemical changes depicted in **Figure 1.5**.

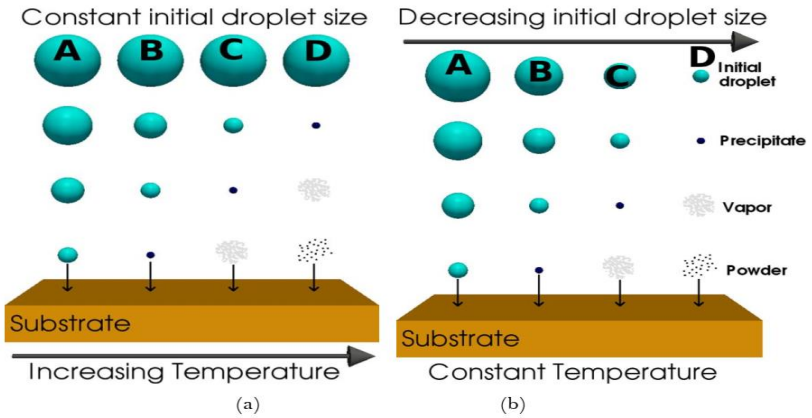

Figure I.5. Diagram of the different process stages for the aerosol droplet evolution as it approaches the hot substrate for two cases [6].

As the droplet traverses the ambient, there are four forces simultaneously acting on it, describing its path. Those forces are gravitational, electrical, thermophoretic, and the Stokes force. As shown in Figure I.6.The thermos-phoretic force pushes the droplets away from a hot surface, because the gas molecules from the hotter side of the droplet rebound with higher kinetic energy than those from the cooler side. For example, at a surface temperature of 350°C and a thermal gradient of 500 °C/cm it was calculated that the thermophoretic force is equal to the gravitational force for a droplet of 2 μm in diameter. Thermophoretic forces keep most droplets away from the surface in non-electrostatics pray process. It was concluded that the film grows from the vapor of droplets passing very close to the hot substrate in a manner of chemical vapor deposition **(Figure I.6)**. Drop lets that strike the substrate form a powdery deposit. The authors suggest that forcing droplets closer to the substrate while avoiding actual contact would improve the efficiency of film growth.

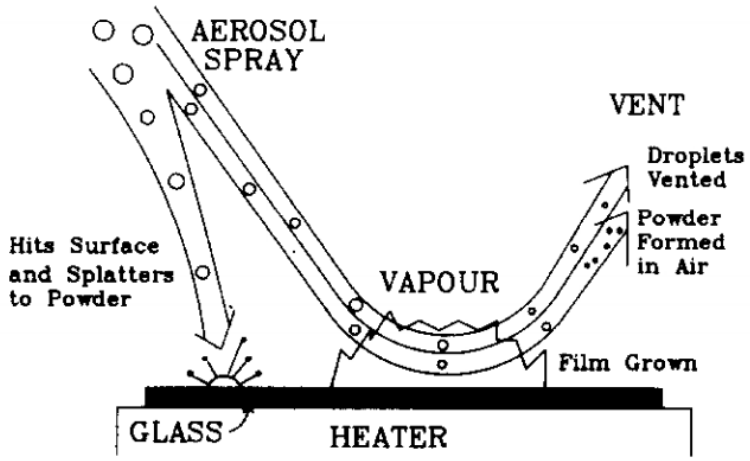

Figure I.6. The interaction of an aerosol spray with a hot substrate showing a proposed mechanism of film [19]

I.4.3.3. Precursor Decomposition

The precursor, as it moves through the heated ambient under goes various changes, which are characterized in **Figure I.6**.Evaporation, precipitate formation, and vaporization all occurred pending on the droplet size and ambient temperature. Figure I.6 shows the four physical forms in which the droplet may interact with the substrate surface. Although all processes occur during deposition, process C, the CVD-like deposition is desired to yield a dense high-quality film [12].

When the processing environment causes droplets to evaporate prior to reaching the substrate vicinity, a precipitate will form early. As the precipitate reaches the immediate vicinity

of the substrate, it is converted into a vapor state and it undergoes a heterogeneous reaction through the following steps :

1. Reactant molecules diffuse to the surface.
2. Adsorption of some molecules at the surface.
3. Surface diffusion and a chemical reaction, incorporating the reactant into the lattice.
4. Desorption and diffusion of the product molecules from the surface [8].

I.4.4. Quality of the deposited films

Thin film's properties and quality are influenced by various parameters prepared by spray pyrolysis, which are :

- The temperature of the substrate.
- The precursor solution
- The distance between the nozzle and the substrate.
- The carrier gas and the rate at which the aerosol passes through.
- The size and opening time of the nozzle.
- The number of sprays.

- The spray method has some disadvantages such as the materials to be deposited must be soluble, Edge effects (greater thickness on the edges of the substrate) and the problem of cleaning the laborious device [20].

I.5. Zinc sulfide properties

ZnS compound is one of the most important semiconductor material, and it has been largely investigated in the recent years due to the wide band gap (3.7 eV), non toxicity, safety to environment and high transparency of ZnS, it can be useful for extensively applications in optoelectronic devices, such as light-emitting diode and laser diode from blue to ultraviolet band, fluorescence and electroluminescence thin film devices and n-type window material in solar cell, [21], and it also can e used as a reflector and dielectric filter because of its high refractive index (2.35) and its high transmittance in the visible range, respectively [22].

I.5.1. Main characteristics

I.5.1.1. Structural properties

ZnS is found in nature in the mineral of sphalerite. It has commonly two available allotropes : the *zinc blende* (ZB) cubic form, which is more stable, and the *wurtzite* (WZ) hexagonal form. The ZB structure results in tetrahedrally coordinated zinc and sulfur atoms stacked in the ABCABC pattern, while the WZ form has the same structure with atoms stacked

in the ABABAB pattern, **Figure I.7** *(a)* and *(b)* shows the view of the ZB and WZ structures, respectively. The lattice parameters of WZ are $a = b = 3.82$ Å, $c = 6.26$ Å and those of ZB are $a = b = c = 5.41$ Å. The energy gap difference between the two structures is about 0.05 eV [23].

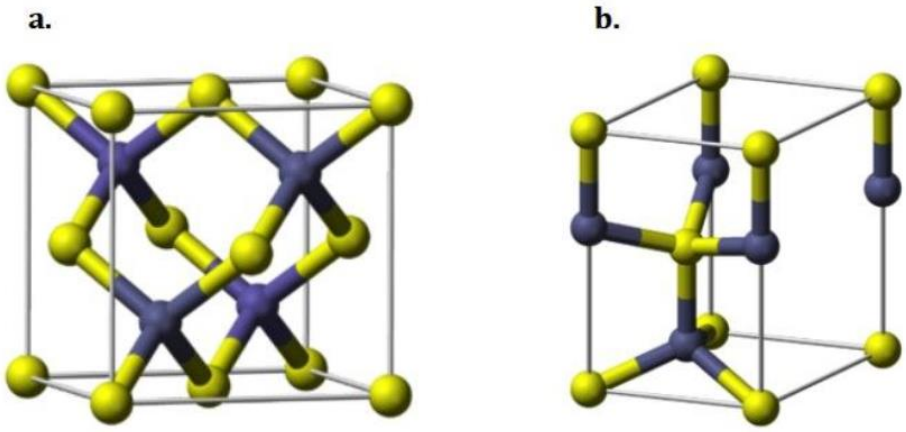

Figure I.7. Schematic view of the zinc blende (a) and wurtzite (b) crystal structures for the zinc sulfide [23]

Table I.3 Physical properties of fundamental ZnS structure [24].

SN	PROPERTY	ZnS	
		Zinc Blende	Wurtzite
1	Lattice parameters (at 300k)	a= 0.541nm	a= 0.3811 nmc= 0.6234nm
2	Density (at 300k)	4.11 g.cm^{-3}	3.98 g.cm^{-3}
3	Dielectric constant	8.9	9.6
4	Refractive index	2.368	2.356/2.378
5	Energy Gap E_g (at 300k)	3.68	3.91
6	Exciton binding energy (meV)	39	39
7	Positions of UV emissions	330-345nm	330-345nm

I.5.1.2. Optical properties

Zinc sulfide has a high refractive index of about 2.35 at wavelength of 632 nm [23], **Figure I.8** *(a)* and *(b)* show the transmittance and the absorbance, respectively, of ZnS thin films deposited by Successive Ionic Layer Adsorption and Reaction (SILAR) at different annealing temperatures. The absorbance is low in the visible and near infrared regions, but is

high in the UV region, with an enhanced absorption observed close to 360 nm. The transmittance is very high in the visible and near infrared regions, and low in the UV region. The high transmittance of about 90 % in the visible range show in **Figure I.8** *(a)* leads to the conclusion that the ZnS films are actually efficient transmitting and antireflective materials. **Figure I.9** *(a)* shows the plot of $(\alpha hv)^2$ (where α is the optical absorption coefficient and hv is the energy of the incident photon) as a function of the photon energy. **Figure I.9** *(b)* shows the energy gap as a function of the temperature.

The decrease in energy gap with increasing annealing temperature could be attributed to improvement in the crystal quality or to possible variation of the grain size [25].

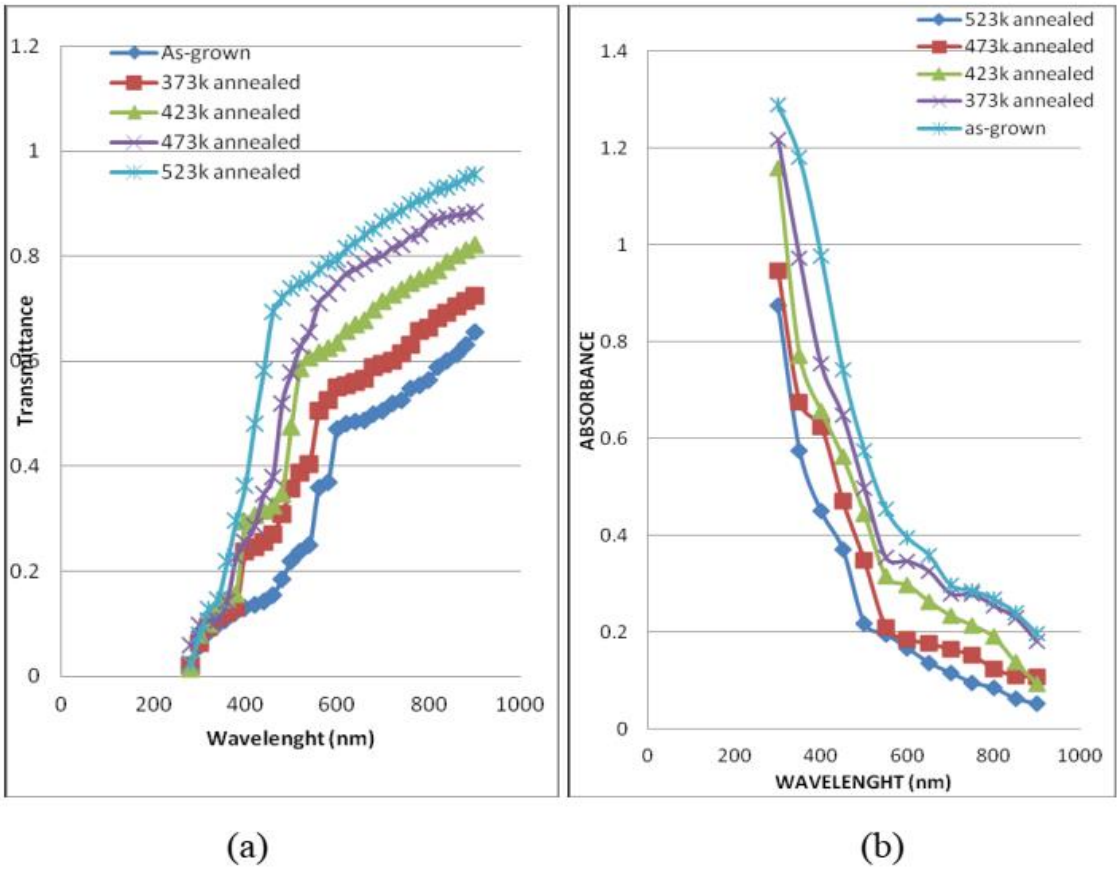

Figure I.8. Transmittance (a) and absorbance (b) as a function of the wavelength for ZnS thin films deposited by SILAR at different annealing temperatures *[25]*

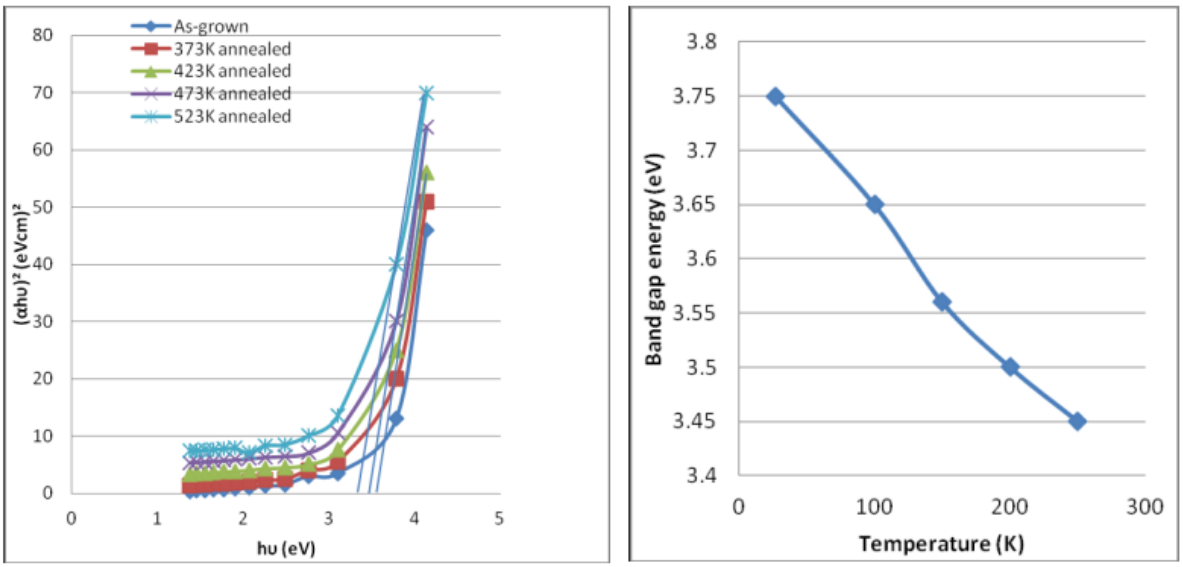

Figure I.9. $(\alpha h\nu)^2$ as a function of the photon energy (a) and energy gap as a function of temperature (b) for ZnS thin films deposited by SILAR at different annealing temperatures [25]

I.5.1.3. Electrical and Dielectric properties

ZnS, well-known direct band gap II–VI semiconductor, is promising materials for electronic devices and due to it's wide band gap it has attracted particular attention in recent years [24]. At room temperature Zinc sulphide has been taken in zinc blended with a band hole at 3.6 eV. The band hole is3.7701 eV. Zincsulphide with a band hole of 3.68 eV compares to vivid rays for visual inter-band progress. Extensive-band hole semiconductors, for example, Zinc-Sulphide are ideal materials for the analysis of isolated states in the hole [26].

Dielectric studies show that the conduction phenomenon in ZnS nanostructures depends on the temperature and the frequency of the external electric field applied. The dielectric constant decreases with an increase in the frequency. In addition, it results much higher than that of the bulk ZnS, which can be treated as an insulator [27].

I.5.2. Applications of ZnS

Zinc Sulphide has a potential application in field emission of electron induced by external electromagnetic field. The large work function of ZnS (7.0eV) other than materials like Si (3.6eV) ZnO (5.3eV) makes it a good candidate for field emitting material. It was established that ZnS exhibited enhanced field emission properties such as emission current, stability, turn on field and field enhancement factors. Filed emitters have great applications in high brightness electron sources, flat panel displays and microwave devices.

Also, due to its chemical stability against oxidation and hydrolysis when exposed to violent environment, zinc sulphide are interesting materials for catalytic application. They can be used as important catalyst in environmental protection by removing organic and toxic water pollutants. They have also be used for the photocatalytic degradation of organic pollutant such as dyes halogenated benzene derivatives in waste water treatment.

Zinc Sulphide is considered important for application in light emitting diodes (LEDs). The properties of LEDs such as its high efficiency, low power consumption environmentally friendly, long lifetimes, fast response to time etc and their optical properties such as broad absorption easy control of the emission and superior luminescence efficiency have made it an attractive choice for the next generation of displays.

Other applications of zinc sulphides includes its use in Sensors, Laser Solar, Solar Cells, Cell imaging, amongst others [15].

I.6. Thin film characterization techniques

I.6.1. X- Ray Diffraction (XRD) Technique

Diffraction is a phenomenon by which X-rays are reflected from the atoms in a crystalline solid. The diffracted X-rays create a pattern that shows the structural orientation of each atom in a given compound.

When monochromatic X-rays affect upon the atoms in a crystal lattice, each atom acts like source of scattering. As shown in the schematic representation in **Figure I.10**, the crystal lattice functions as group of parallel reflecting planes. The intensity of the reflected rays reaches the maximum at particular angles (constructive interference) when the path difference between two reflected waves from two different planes in an integral multiple of the X-rays' wavelength λ. This is known as Bragg's law that is presented by the following relation :

$$2d\sin\theta = n\lambda \qquad \text{(I.3)}$$

Where : d is the interplanar spacing, θ is the diffraction angle, λ is the wavelength of x-ray and n is the order of diffraction [28].

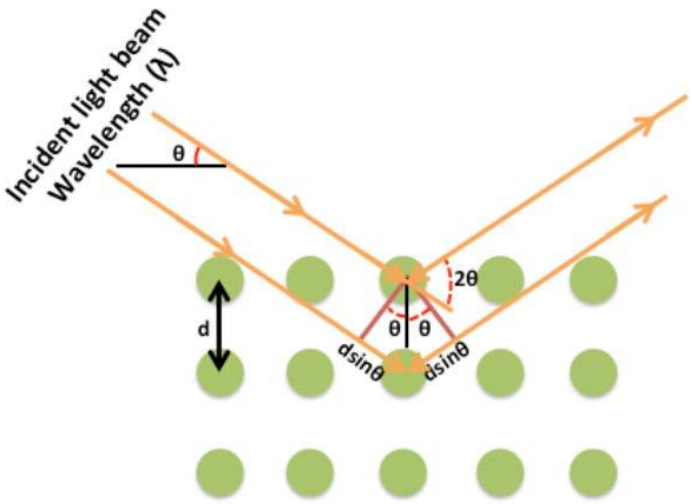

Figure I.10. Schematic description of Bragg's Diffraction Law [28].

This technique allows to obtain a lot of information about the samples: crystallization, presence of parasitic phases, crystallographic parameters, orientation, grain size and the residual stresses ect [29].

I.6.2. Scanning Electron Microscopy (SEM)

Scanning electron microscopy SEM is one of the most used instruments in research areas and semiconductor industries due to its large depth of field which allows a large amount of the sample to be in focus at one time and produces an image that is a good representation of the surface topography and due to its high resolution, which makes possible the examination of features at high magnification. It is also a non-destructive technique that provides information on the morphology of the sample, its mode of crystallization, sometimes to estimate the crystallites sizes and the thickness of the sample from cross sectional view [29].

The SEM uses a high energy electron ray by electron guns in order to get high resolution images of the sample surface. This ray is quickened towards the samples (with a positive electrical potential) while is concentrating using metal apertures and electromagnetic lenses. In the last lens, the SEM consists of groups of coils which permit to deflect the electron beam back and forth through the sample (**Fig I.11**). The formation of secondary electrons back scattered electrons, characteristic and continuum x-rays, Auger electrons and photons of various energies are a result of bombardment of the sample surface with high energy electrons [28].

For the electrons to be able to pass through the sample, the sample should be conductive. In case of a non-conductive sample a layer of a conductive material such as gold is sputtered on the surface of the sample [30].

The main impacts on the electrons of a beam impinging the sample is elastic scattering (the loss of energy is negligible with change of direction) and inelastic scattering (energy loss with negligible change of direction). The major cause of elastic scattering is the interactions with the atoms' nuclei and lead to important deviations from the direction of the incident beam. Inelastic scattering results from two mechanisms, inelastic interaction with the atomic nucleus and inelastic interaction with the tied electrons. The moving electron frees energy in the Coulomb field of the nucleus and sends white or continuum x ray radiation when inelastic scattering happens through interaction with the atomic nucleus. Energy is transferred from the electron beam to the loosely bound electron which is emitted if inelastic scattering happens among a loosely bound electron on an outer shell of the atom and an electron of the incident ray. The electrons emitted through this process are called secondary electrons. Nevertheless, these electrons are generally recollected by ionized atoms in the sample [28].

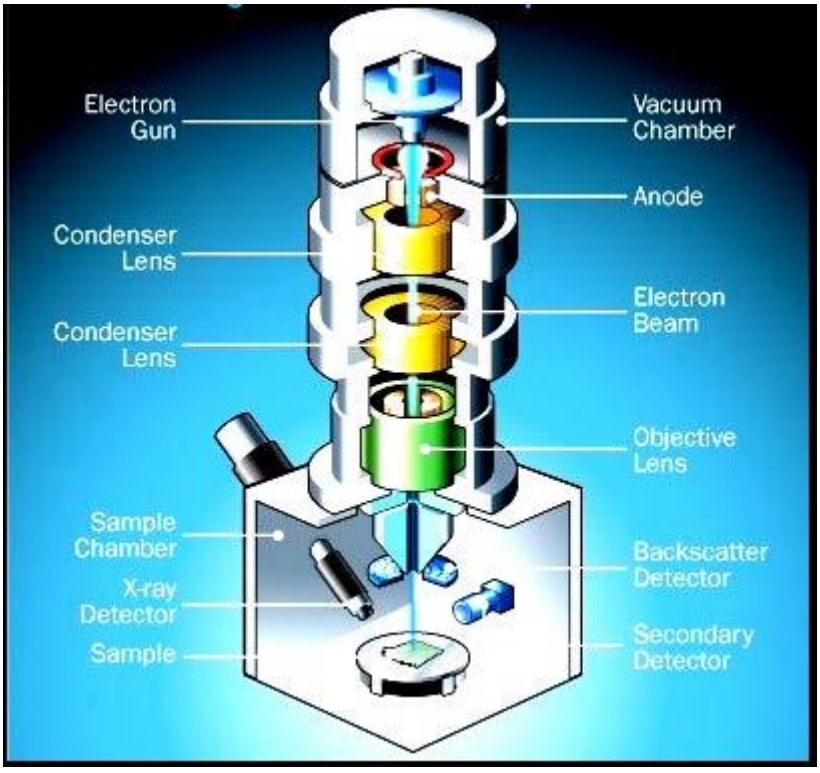

Figure I.11. Schematic representation of scanning electronic microscopy [28].

I.6.3. Energy Dispersive Spectroscopy

Energy-dispersive spectroscopy (EDS or EDX) are commonly paired with SEM equipment as the same principle for sample analysis is used. It is an analytical technique used for the elemental analysis of a sample. Its characterization capabilities are due in large part to the fundamental principle that each element has a unique atomic structure allowing X-rays that are characteristic of the element's atomic structure to be identified uniquely from one another.

These characteristic X-rays occur when the electrons from the electron beam strike the electrons of an inner orbital of the specimen's atom. The force of this strike will knock the electron out of the orbitals of the atom and becomes a "free" electron. The ionized atom then compensates for this by adjusting and electrons from higher orbitals begin to drop down to lower orbitals releasing energy in several forms, including X-rays. Realesed X-ray photon energy is equal to the energy difference between the two levels involved. The X-ray released by the electron is then detected by a solid state detector and converted into signals which are processed into an Xray energy spectrum.

Thus, by measuring the amounts of energy present in the X-rays being released by a specimen during electron beam bombardment, the identity of the atom from which the X – ray was emitted can be established. Characteristic x-rays from each element are used to determine the concentrations of the different elements in the specimen. Each of these peaks is unique to an atom and therefore corresponds to a single element. The higher a peak in a spectrum, the more concentrated the element is in the specimen.

There are a couple of things to note about EDS, EDS is not a surface analysis but instead a volume analysis. This is important for evaluating thin films as thi depth is often larger than the thickness of the thin film. That means that elements from the substrate will be detected and must be accounted for. Second, the peaks produced by EDS must be evaluated with care [31].

I.6.4. Spectrophotometry

UV-Visible spectrophotometry is an optical characterization method used to study the optical properties of a material such as the transparency, the refractive index, extinction coefficient, energy gap, etc., from the detection of the transmitted (T), absorbed (A) or reflected (R) radiation. These are the three possible radiation when an incident beam of intensity strikes a sample. According to the frequency of the incident radiation, the radiation-matter interaction involves various types of energy levels of matter. The involved energies have the same magnitude order as molecule binding energies, and this radiation can also cause bond breaks. More generally, they cause electronic transitions between the different energy levels of molecules. The type of obtained information will depend on the sensitivity apparatus and the nature of the sample [29].

There are two types of spectrophotometer which can be used for measuring the transmission in low absorbing materials :

- ***Single beam spectrophotometer*** : The schematic diagram of a single-beam spectrophotometer is shown in Fig. 1. Light from the source lamp is collimated and then passed through a monochromator, which diffracts the light. The narrow bandwidths of this diffracted spectrum are then passed through a mechanical slit on the output side of the monochromator. Then the intensity of the light transmitted through the sample is measured by detectors and converted to absorbance or transmittance.
- ***Double beam spectrophotometer*** : It overcomes certain limitations of the single beam spectrophotometers and is therefore preferred over them. A double beam spectrophotometer has two light beams, one of which passes through the sample while other passes through a reference cell as shown in Fig. 1. This allows more reproducible measurements as any fluctuation in the light source or instrument electronics appears in both reference and the sample and therefore can easily be removed from the sample spectrum by subtracting the reference spectrum.

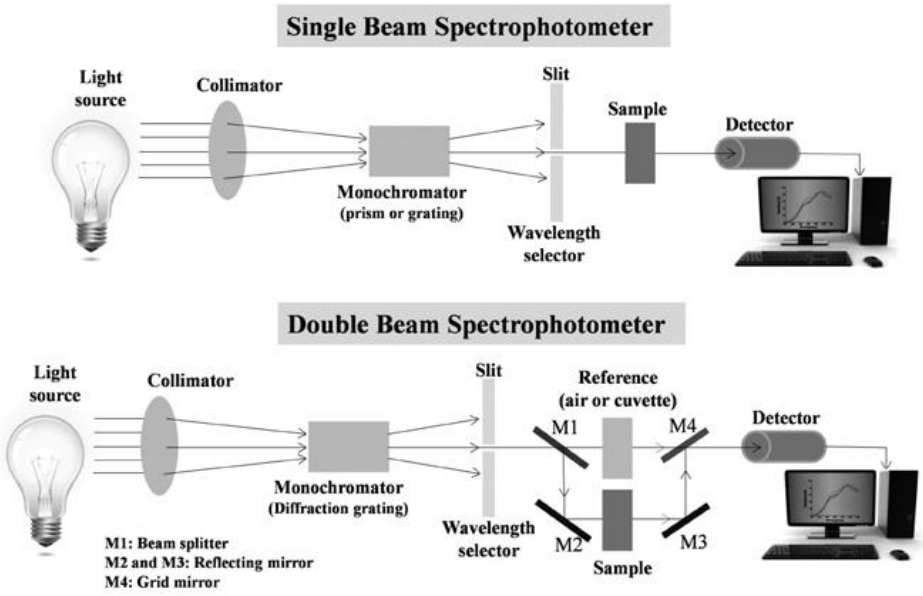

Figure I.12. Schematic of Single and double beam spectrophotometer [32].

For transmission measurements in thin film samples, the spectrophotometer quantitatively compares the fraction of light that passes through a reference and the thin film, then electronically compares the intensities of the two signals and computes the percentage of transmission of the sample compared to the reference [32].

I.6.5. Hall effect

Experimental study of the Hall effect is an effective method to investigate the motion of charge carriers in metals and semiconductors. Moreover, the Hall effect gives information about concentration of charge carriers and nature of semiconductor's conductivity [33].

When an electron moves, under the effect of an electric field, along a direction perpendicular to an applied magnetic field $\vec{B}$, it undergoes a force $\vec{F}$ (called the Lorentz force) perpendicular to the plane formed by its trajectory and $\vec{B}$. As illustrated in a **Figure I.13**, the electrons deviate to one side of the thin conductor which causes a potential between the two sides of the sample. This measurable transverse voltage is called the Hall Effect (VV_{HH}) after E.H. Hall who discovered it in 1879 [28].

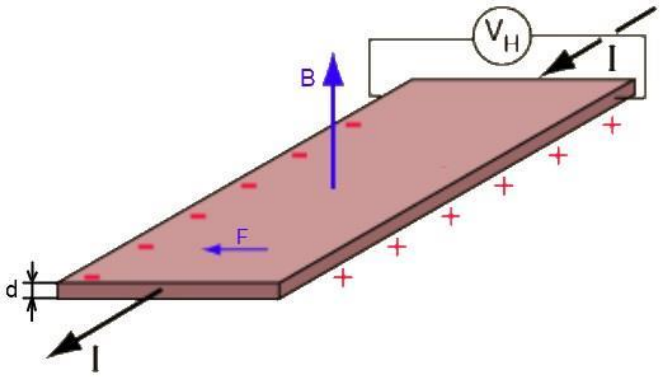

Figure I.13. Schematic illustration of the Hall effect [28].

While the Hall effect was discovered in a metal, today it is used mainly for the characterization of semiconductors, both of single crystals as well as of thin films. From the measured Hall voltage VH the carrier density of a single crystal or a thin film can be calculated. By measuring simultaneously, the conductivity on the same sample also the so-called Hall mobility mH of the charge carriers can be determined [34].

References

[1] M. Bereznai, *Thin film deposition in nitrogen and argon background gases by pulsed laser ablation of molybenum, tungsten, carbon and boron-carbid target materials, PhD theses, University of Szeged,* 2011.

[2] K. K. Schuegraf, HANDBOOK OF THIN-FILM DEPOSITION PROCESSES AND TECHNIQUES. Eaton Avenue Norwich, NY 13815 1-800-932-7045.Krishna Seshan(2nd edition)., 2002.

[3] Y. Salah, *L'effet de la molarité des différentes sources d'étain sur les propriétés des couches minces d'oxyde d'étain SnO2 élaborées par Spray Ultrasonique, Université Mohamed Khider - Biskra,* 2014.

[4] X. Li, M. Rui, J. Song, Z. Shen and H. Zeng, *Advanced Functional Materials 25, 4929,* 2015.

[5] M. Khachane, *Étude des matériaux ferroélectriques céramiques et couches minces à base de nimbâtes alcalino-terreux et multicouches ferroélectriques-catalytiques pour capteur de gaz, Thèse doctorat. Université du Sud Toulon- Var.,* 2007.

[6] G. Mebrouk, *Elaboration and characterization of nanostructuring NiO thin films for gas sensing applications, doctorate thesis, University of Mohamed Khider, BISKRA.,* 2019.

[7] Olayinka Oluwatosin Abegunde, Esther Titilayo Akinlabi, Oluseyi Philip Oladijo, Stephen Akinlabi, Albert Uchenna Ude, «Overview of thin film deposition techniques,» *AIMS Materials Science,* vol. 6, n° %12, p. 176, 2019.

[8] Guechi Amira, Boutaghou Wissam, *STRUCTURAL, OPTICAL AND ELECTRICAL PROPERTIES OF (Al/CuO/ZnO) AND (Al/CuO/SnO2) HETEROSTRUCTURES PREPARED BY SPRAY PYROLYSIS INTENDED FOR THE PHOTODETECTION OF ULTRAVIOLET LIGHT, Master thesis, UNIVERSITY LARBI BEN M'HIDI UNIVERSITY, OUM EL BOUAGHI,* 2022.

[9] E. Acosta, Thin Films, 2021.

[10] F. BOUAICHI, *Deposition and analysis of Zinc Oxide thin films elaborated using spray pyrolysis for photovoltaic applications, doctorate thesis, University Mohamed Khider, Biskra,* 2019.

[11] A. Mockutė, *Thin Film Synthesis and Characterization of New MAX Phase Alloys, Linköping University, sweden,* 2013.

[12] D. PEREDNIS, *Thin Film Deposition by Spray Pyrolysis and the Application in Solid Oxide Fuel Cells*, 2003.

[13] Saeed Rahemi Ardekani, Alireza Sabour Rouh Aghdam, Mojtaba Nazari, Amir Bayat, Elnaz Yazdani, Esmaiel Saievar-Iranizad, «A comprehensive review on ultrasonic spray

pyrolysis technique: Mechanism, main parameters and applications in condensed matter,» *Journal of Analytical and Applied Pyrolysis, ELSEVIER*, vol. 141, n° %1104631, 2019.

[14] Lado Filipovic, Siegfried Selberherr, Giorgio C. Mutinati, Elise Brunet, Stephan Steinhauer, Anton Köck, Jordi Teva, Jochen Kraft, Jörg Siegert, Franz Schrank, «Methods of simulating thin film deposition using spray pyrolysis techniques,» *Microelectronic Engineering*, vol. 117, pp. 57-66, 2014.

[15] S. I. Okpara, *DEPOSITION AND PROPERTIES OF ZNS:MN THIN FILMS AND NANOSTRUCTURED LAYERS BY SPRAY PYROLYSIS METHOD, MASTER THESIS, Tallinn University*, 2018.

[16] P. S. Patil, «Versatility of chemical spray pyrolysis technique,» *Materials Chemistry and Physics*, vol. 59, p. 185–198, 1999.

[17] Dae Soo Jung, Seung Bin Park, Yun Chan Kang , «Design of particles by spray pyrolysis and recent progress in its application,» *Korean Journal of Chemical Engineering*, vol. 27, pp. 1621-1645, 2010.

[18] D. PEREDNIS, *Thin Film Deposition by Spray Pyrolysis and the Application in Solid Oxide Fuel Cells, doctorate thesis, SWISS*, 2003.

[19] W. M. SEARS, MICHAEL A. GEE, «Mechanics of film formation during the spray pyrolysis of tin oxide,» *Thin solid films* , vol. 165, pp. 265-277, 1988.

[20] N. ABDELOUAHAB, *Preparation and characterization of thin films nanostructures based on ZnO and other oxides, doctorate thesis, LARBI BEN M'HIDI UNIVERSITY, OUM EL BOUAGHI.*

[21] A. Derbali, A. Attaf, H. Saidi, H. Benamra, M. Nouadji, M.S. Aida, N. Attaf, H. Ezzaouia, «Investigation of structural, optical and electrical properties of ZnS thin films prepared by ultrasonic spray technique for photovoltaic applications,» *Optik*, vol. 154, p. 286–293, 2018.

[22] B. Elidrissi, M. Addou, M. Regragui, A. Bougrine, A. Kachouane, J.C. Bernède, «Structure, composition and optical properties of ZnS thinfilms prepared by spray pyrolysis,» *Materials Chemistry and Physics*, vol. 68, p. 175–179, 2001.

[23] A. Bartolucci, *Morphological characterization of ZnS thin films for photovoltaic applications, ALMA MATER STUDIORUM · UNIVERSITÀ DI BOLOGNA*, 2015.

[24] *ZnS nanoparticles – Synthesis, Characterization & Application, Delhi Technological University*, 2013.

[25] A.A. Ibiyemi, A.O. Awodugba, «The Influence of Annealing on Electrical and Optical Properties of ZnS Thin Film,» *The Pacific Journal of Science and Technology*, vol. 13(1), pp. 213-220, 2012.

[26] S. D. S, *SYNTHESIS AND CHARACTERISATION OF ZINC SULPHIDE NANOPARTICLES*, 2019.

[27] S. Suresh, «Synthesis, structural and dielectric properties of zinc sulfide nanoparticles,» *International Journal of Physical Sciences* , vol. 8, n° %121, pp. 1121-1127, 2013.

[28] B. KHEIRA, *Elaboration and characterization of SnO2:In thin films deposited by spray pyrolysis technique, Doctorate thesis, University Mohamed Kheider of Biskra,* 2020.

[29] A. BOUKHARI, *Elaboration, characterization and modeling of oxide-based nanostructured thin films, doctorate thesis, University of M'sila,* 2021.

[30] S. Azhar, *Synthesis of well defined hematite films and their use for sintering studies, master thesis, Lulea University*, 2007.

[31] W. Allag, *Study of thin films for photovoltaic solar cells, doctorate thesis, FERHAT ABBAS UNIVERSITY – SETIF -1-*, 2022.

[32] S. Jena, R.B. Tokas, S. Thakur, N.K. Sahoo, «Characterization of Optical Thin Films by Spectrophotometry and Atomic Force Microscopy,» *SMC Bulletin*, vol. 6, n° %11, 2015.

[33] K. Kuzmina, *Quantum Hall effect in 2 dimensional GaInAs structure, master thesis, Lappeenranta unversity,* 2013.

[34] K. ELLMER, «HALL EFFECT AND CONDUCTIVITY MEASUREMENTS IN SEMICONDUCTOR CRYSTALS AND THIN FILMS,» *Characterization of Materials*, pp. 565-579, 2012.

Chapter II : Solar cells technology

II.1. Introduction

One of the pillars of the modern and growing society is energy [1], so the very important goal nowadays is to find a new renewable form of energy, The renewable sources of energy derived from the sun are one of the promising options [2]. Sun provides enormous amounts of energy powering oceans, atmospheric currents, and cycle of evaporation and drives river flow, hurricanes and tornadoes that destroy natural landscape.

Earth's resource of oil mounts up to 3 trillion barrels containing $1{,}7 \cdot 10^{22}$ joules of energy that the sun supplies in 1,5 days. Humans annually use about $4{,}6 \cdot 10^{20}$ joules annually which sun supplies in one hour. The sun continuously supplies about $1{,}2 \cdot 10^{25}$ terawatts of energy which is very much greater than any other renewable or non renewable sources of energy can provide. This energy is much greater than the energy required by human beings which is about 13 terawatts [3].

As the importance of solar cells in different technologies increases, there is a need to enhance their reliability and efficiency [4].

This chapter lays out the most important informations on solar cells, the basics of it's work, those cells characteristics and different generations.

II.2. Principles of solar cells

II.2.1. Solar Spectrum

The study of solar cells (progress, optimization and characterization….etc.) need some information about the source of energy used; the sun. This star is the biggest member of the solar system. The sun is a big sphere of plasma composed of *H* and *He* and some small amounts of other elements, it has an effective black-body temperature *TS* of *5777 K*. The diameter of the sun is around 1.39×10^9 m and the distance between it and the earth is about 1.5×10^{11} m. The solar radiation is partially absorbed and scattered by its passage through the atmosphere. The absorption of the *X*–rays and extreme ultraviolet radiations of the sun is principally caused by nitrogen and oxygen while the absorption of the ultraviolet ($\lambda < 0.40\ \mu m$) and infrared radiations ($\lambda > 2.3\ \mu m$) is mainly caused by the ozone and water vapors. The atmosphere of the earth absorbs the ultraviolet (*UV*) and far infrared radiation and allows only short wavelength radiation (i.e. between *0.29* μm and *2.3* μm). It does not permit radiation having wavelength $\lambda > 2.3\ \mu m$, (i.e. long wavelength radiation) [5].

The wavelength distribution of the sunlight (power per unit area and per unit wavelength) follows approximately the radiation distribution of a black body at this temperature as shown in **Figure II.1**. The total energy per unit area integrated over the entire spectrum and measured outside the atmosphere perpendicular to the direction of the sun is essentially constant. This radiation power is referred to as the solar constant or air mass zero (AM0) radiation [4]. Outside the atmosphere the spectrum is *AM0* and that on the surface of the earth for normal incidence is *AM1* [2].

$$AM = 1/\cos(\theta) \qquad \text{(II.1)}$$

The θ represents the angle of the sun to the vertical [4].

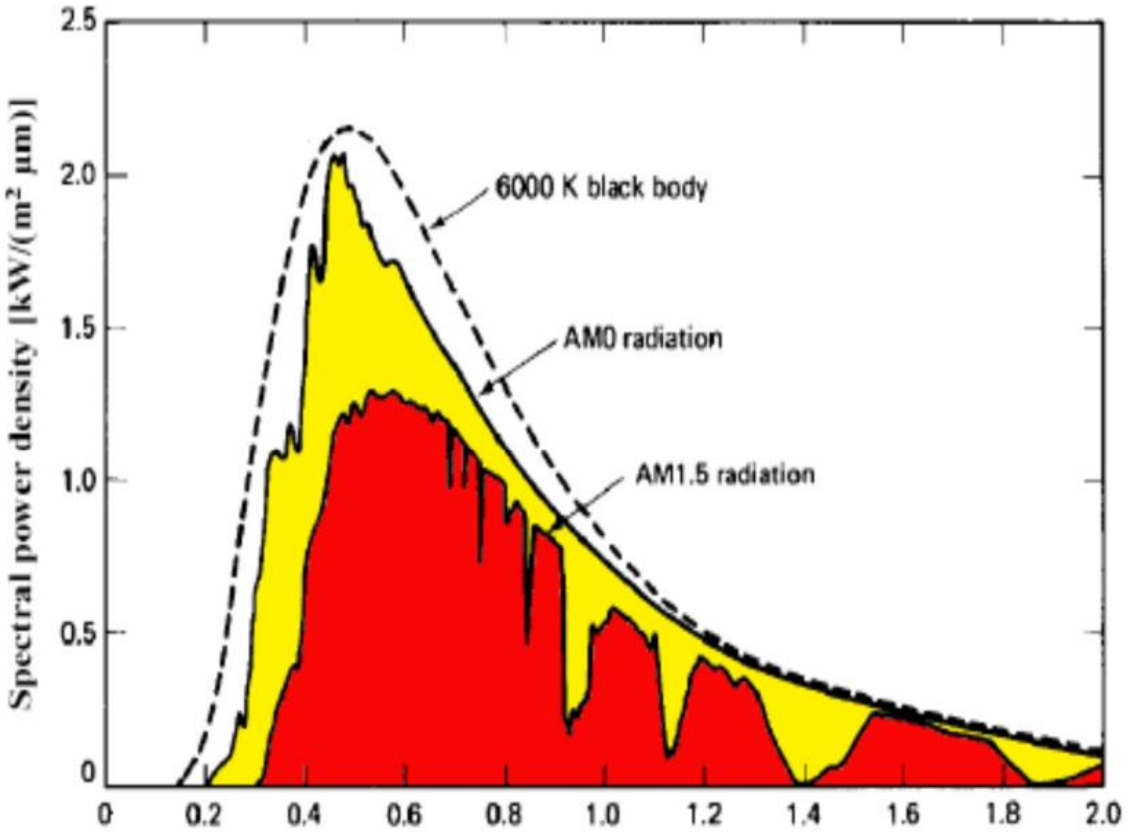

Figure II.1. Spectral power density of sunlight showing AM0 (extraterrestrial radiation), AM1.5 (terrestrial) and the black body radiation at 6000 K [6]

When the solar radiation passes through the earth's atmosphere, the spectral distribution is attenuated and changed as a result of absorption and scattering phenomena in the gas, water and dust. Atmospheric absorption is commonly caused by ozone (O_3), oxygen (O_2), nitrogen (N_2), carbon dioxide (CO_2), carbon oxide (CO) and water vapour (H_2O) while scattering is

mostly caused by aerosols, air molecules (Rayleigh scattering), dust and water droplets (**Figure II.2**) [7].

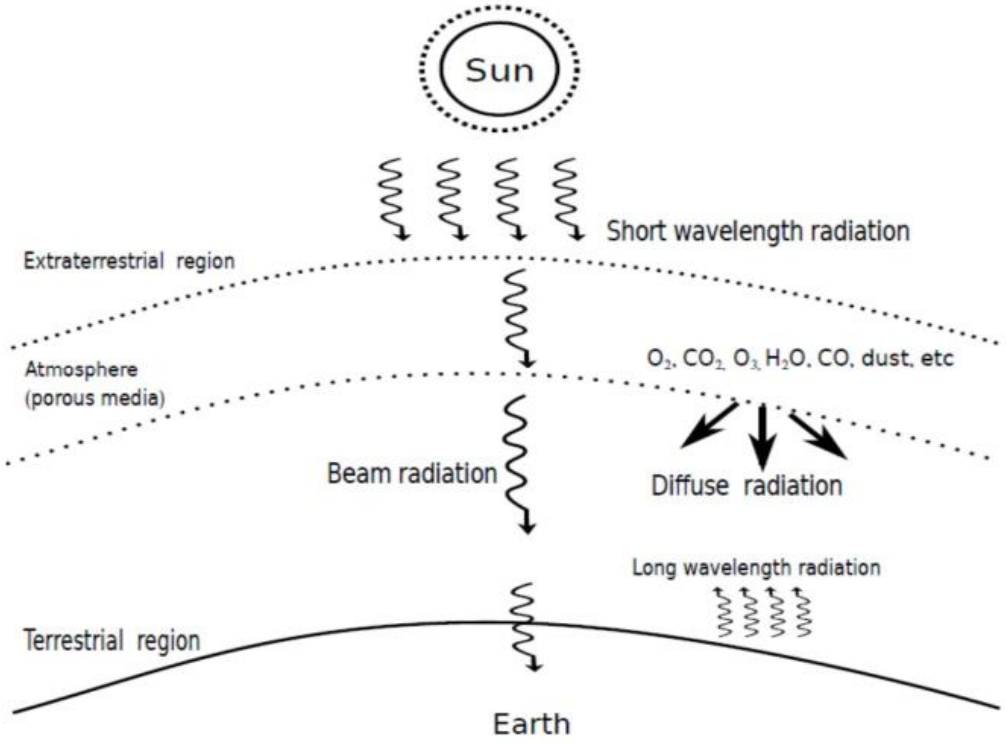

Figure II.2. Terrestrial, extra-terrestrial regions and atmospheric effects [7]

II.2.2. Basic Principles of a Solar Cell

II.2.2.1. The photovoltaic effect

The photovoltaic solar cells are materials able to convert directly the light into electricity, this conversion, called the photovoltaic effect. The origin of the word "photovoltaic" is made up from the Greek word phos (light), and voltaic (electrical) from the name of Italian physicist Alessandro Volta [4]. This effect was first observed by Henri Becquerel in 1839 [2].

The photovoltaic effect is the basic physical process through which a solar cell converts sunlight into electricity. Sunlight is composed of photons (like energy accumulations), or articles of solar energy. These photons contain various amounts of energy corresponding to the different wavelengths of the solar spectrum. When photons hit a PV cell, they may be reflected or absorbed. Only the absorbed photons generate electricity. When this happens, the energy of the photon is transferred to an electron in an atom of the cell. The electron is able to escape for its normal position associated in the atom to become part of the current in an electrical circuit [4].

II.2.2.2. The P-N junction

The solar cells require to realise two steps: the first, is the photogeneration of charge carriers (electrons and holes) and secondly the separation of these carriers to a conductive contact that will transmit the electricity. Currently, the majority of solar cells in use are silicon semi-conductor junction devices. Therefore, in order to study the photovoltaic cells we must have an understanding of the basics of the semi-conductor materials and particularly the *PN* junction [8].

The most predominant semiconductor material currently used in solar cells is Silicon. It is abundant, and its material properties have been extensively studied. Silicon (Si) is a group IV element which alludes to the four valence electrons of an isolated Si atom has in its outer shell. When in the vicinity of other Si atoms these valence electrons are shared to form covalent bonds between atoms in order to fill the atoms outer shells. These bonds allow for the formation of orderly crystal structures.

If a Silicon atom is replaced with another type of atom, such as a group III material (Boron atom for example) that only has three valence electrons, there will be a Silicon atom that does not have four electrons it can share. The vacancy results in a hole that easily accepts a free electron. If more Silicon atoms are replaced, there will be more holes. The resulting material is called p-type. If the Silicon atom was instead replaced with a group V material (Arsenide atom for example) that has five electrons in its outermost shell, there is instead an extra electron. Since this electron is not tightly bound, it is free to move throughout the material, making it n-type.

A p-n junction is a semiconductor junction where a p-doped region is in contact with a n-doped region as seen in **Figure II.3**. Where an n-type semiconductor comes into contact with a p-type semiconductor, a p-n junction is formed. In p-n junctions the p-side and n-side can be made from different semiconductors, which are called heterojunctions, or the p-side and n-side can be differently doped regions of the same material, which is called homojunctions [9].

Once the two semiconductors are in contact, electrons from the nregion near the junction interface diffuse in the p-region leaving donor atoms electrically unshielded by the majority carriers. In the same way, holes from the p-region near the interface diffuse in the n-region, leaving acceptors unshielded behind. This phenomenon is called “diffusion”. The region nearby the p-n interface, common at the two semiconductors, which lost its neutrality and become actively charged, is called the “space charge region” (SCR). The rest of the two semiconductors

which is not influenced by the metallurgical junction is called "quasi neutral region" (QNR). A schematic of the p-n junction is shown in Figure **II.3** [10]**.**

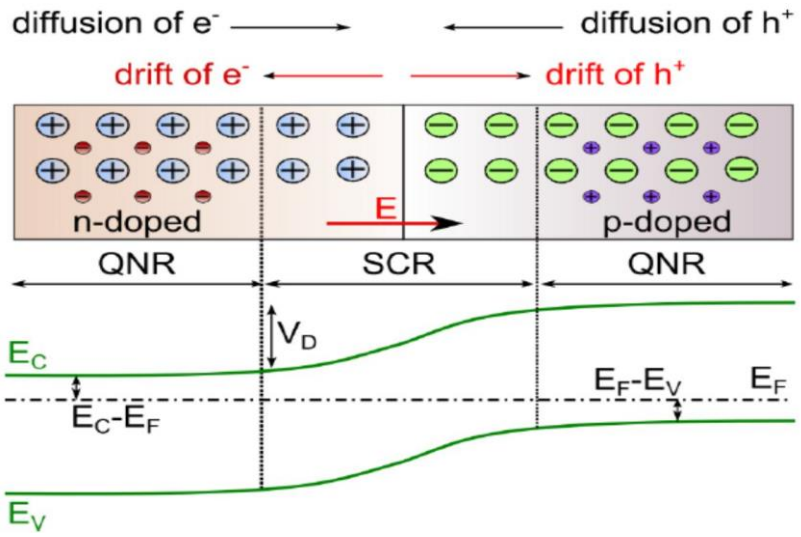

Figure II.3. p-n junction in thermal equilibrium with zero-bias voltage applied [10].

II.2.2.3. Photon-semiconductor interaction

Sunlight is composed of photons (like energy accumulations), or particles of solar energy. These photons contain various amounts of energy corresponding to the different wavelengths of the solar spectrum [4]. The sunlight consists of photons that each has a different energy and wavelength. The relationship between photon energy (E) in electron Volts and the wavelength (λ) of the incident light in micrometers is given as :

$$E(eV) = \frac{1.24}{\lambda(\mu m)} \qquad \text{(II.2)}$$

On the other side, Physics of photovoltaics is based on the optical and electrical properties of semiconductors. A semiconductor is generally characterised by a bandgap energy E_g, the energy needed to create an electron-hole (e-h) pair.

When a photon with energy larger than the bandgap of the semiconductor ($E_{ph}>E_g$) is absorbed, an electron-hole pair is created. This means that an electron is stimulated from the valence band (E_v) to the conduction band (E_c) leaving a hole behind. This pair needs to be separated then by electric field in order to avoid recombination : this field is provided by a p-n junction which is the core of a photovoltaic device. A photon hitting on the surface of a semiconductor could be either reflected from the surface, absorbed in the material or transmitted throughout the material itself. In the case of PV devices, photons which are not

absorbed (thus reflected or transmitted) are typically considered as a loss since they do not generate power. Considering the energy of the photon and the bandgap of the semiconductor it is possible to establish if a photon is absorbed or transmitted:

- If ($E_{ph}<E_g$): The photons pass through the semiconductor without being absorbed (transmitted).
- If ($E_{ph}= E_g$): In this case the photons are absorbed (they have just enough energy to create an electron-hole pair).
- If ($E_{ph}>E_g$): Photons with energy higher than the band gap are also absorbed. However, for PV applications, part of the energy of these photons is released since electrons quickly thermalize down to the E_c lower energy states [9].

II.2.3. Current-voltage characteristics of the solar cell (Equivalent circuit of a solar cell)

The equivalent circuit of a single junction solar cell is shown in **Figure II.4** and it considers an ideal (a) and a real solar cell model (b)

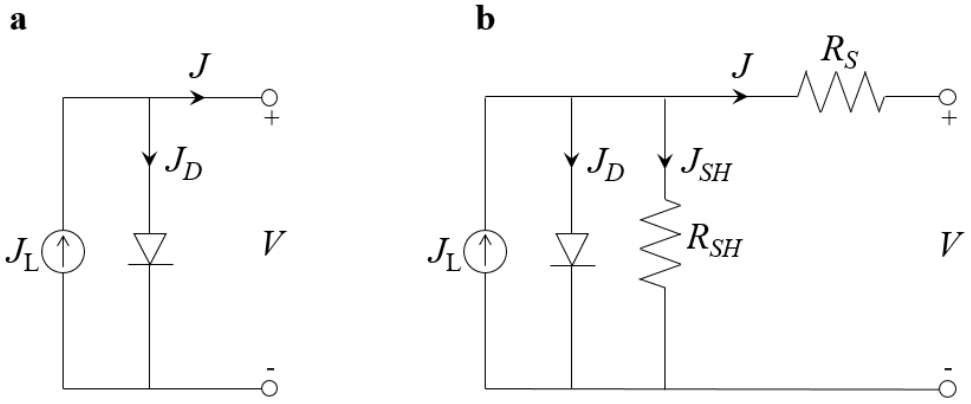

Figure II.4. Equivalent circuit of a) an ideal cell and b) a real (non-ideal) solar cell [11]

Under dark conditions a *p-n* junction can be described using a single diode model, which current – voltage (*I* – *V*) response is given by the Shockley equation. The Shockley equation (Eq II.3) describes the density current (*J*= *I*/area) in an ideal diode :

$$J = J_0(e^{\frac{eV}{nk_BT}} - 1) \qquad \text{(II.3)}$$

where: J_0 is the reverse saturation current, *V* is the voltage across the diode, k_B is the Boltzmann constant, T is the absolute temperature and *n* is the diode ideality factor, a parameter which indicates how close the diode follows the ideal diode equation. The ideality factor is strictly

related to the quality of the solar cell material and the recombination processes, and has typical values between 1 and 2.

In the case of a solar cell however, the diode is connected in parallel to a current source (light) and hence the *J-V* response is:

$$J = J_0(e^{\frac{eV}{nk_BT}} - 1) - J_L \qquad \text{(II.4)}$$

where: J_L is the photocurrent [11].

Note that the photocurrent current is negative because the direction of current flow is, by definition, in the direction opposite to the flow of electrons. Conventionally however, the photocurrent in solar cells is written as a positive current and equation II.5 is also often written in terms of a current density [4] :

$$J = J_L - J_0(e^{\frac{eV}{nk_BT}} - 1) \qquad \text{(II.5)}$$

Real solar cells however, are affected by both shunt (R_{SH}) and series (R_S) resistances as shown in **Figure II.4-b-** which must be taken into consideration in the *J-V* response. Hence, Equation II.4 should be considered:

$$J = J_0(e^{\frac{e(V-AJR_s)}{nk_BT}} - 1) - J_L + \frac{V - AJR_s}{R_{SH}} \qquad \text{(II.6)}$$

where: *A* is the area of the solar cell and $[(V\text{-}AJR_S)/R_{SH}] = J_{SH}$. The resistances act in series (R_S) and in parallel (R_{SH}) with the cell [11].

II.2.4. Solar cell characteristics (parameters)

The main parameters that determine the quality of a solar cell (solar cell figures of merit) are the short circuit current (J_{SC}), open circuit voltage (V_{OC}), and the fill factor (*FF*) are extracted. These values are important as from these it is possible to measure the power conversion efficiency (*PCE* or η) of the solar cell.

A typical *J-V* curve is shown in **Figure II.5**, which shows the main parameters of a solar cell measured in the dark and under illumination. The main parameters for the illuminated *J-V* curve are described as follows:

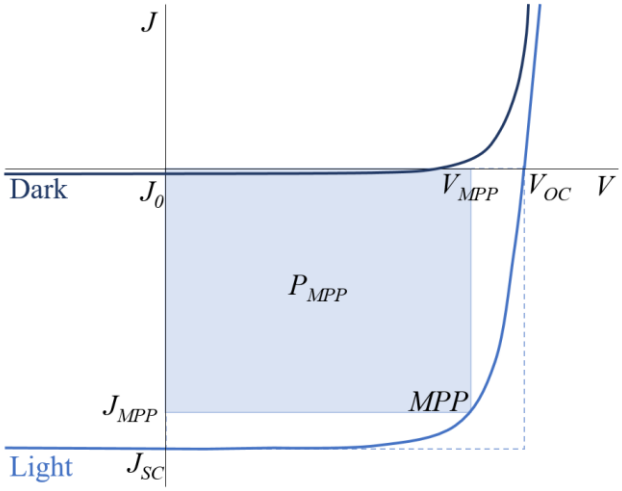

Figure II.5. A J-V curve of a solar cell device under dark and light conditions [11].

II.2.4.1. Short circuit current

The short circuit current Isc is defined as the current through the solar cell when the terminals are in short circuit (i.e., the voltage across the solar cell is zero) [4]. J_{SC} is the current density flowing in the external circuit when the voltage is zero. In an ideal solar cell $J_{SC} = J_L$ [11].

II.2.4.2. Open circuit voltage

Another figure of merit is the open circuit voltage V_{oc}, which is the maximum voltage that the cell can deliver when the current is zero ($J = 0$). The V_{OC} is expressed as follows [11]:

$$V_{OC} = \frac{nk_BT}{e} \ln\left(\frac{J_L}{J_0} + 1\right) \quad \text{(II.7)}$$

II.2.4.3. Fill factor

The fill factor is defined as the ratio of maximum power point $P_m = V_m.I_m$ that can be extracted from a solar cell to the ideal power $P_0 = V_{oc}.I_{sc}$:

$$FF = \frac{V_m.I_m}{V_{OC}.\mathrm{I}_{SC}} \quad \text{(II.8)}$$

The FF is a key parameter in evaluating the performance of solar cells. It is represented in terms of percentage.

II.2.4.4. Efficiency

The conversion efficiency is the most important property of a solar cell. It is defined as the ratio between the generated maximum power, P_m, generated by a solar cell and the incident power, P_{in}, and it is therefore calculated as follows [2]:

$$\eta = \frac{P_m}{P_{in}} = \frac{V_m.I_m}{P_{in}} = \frac{FF.I_{SC}.V_{OC}}{P_{in}} \quad \text{(II.9)}$$

The efficiency of a solar cell can be improved by maximising J_{sc}, V_{oc} and FF. These parameters should be defined under Standard Test Conditions (STM), which are AM 1.5 global spectrum for terrestrial applications, an incident power density of 1000W/m2, and a temperature of 25°C [12].

II.2.4.5. Spectral response and Quantum efficiency

The optical performance of a solar cell can be acquired by a measure of its spectral response (SR) that describes the sensitivity of the solar cell to optical radiation of different wavelengths.

The spectral response is the ratio of the current generated by the solar cell to the power incident on the solar cell. The spectral response is conceptually similar to the quantum efficiency (QE). The quantum efficiency is defined as the number of measured electrons divided by the number of photons, incident on the solar cell.

The quantum efficiency can be determined from the spectral response by replacing the power of the light at a particular wavelength with the photon flux for that wavelength. This gives [13]:

$$SR(\lambda) = \frac{q\lambda}{hc} QE(\lambda) = 0.0808.\lambda.QE(\lambda) \quad \text{(II.10)}$$

It is possible to define two types of quantum efficiency, one is the internal quantum efficiency (IQE) and one is the external quantum efficiency (EQE). They are defined as follows:

- External Quantum Efficiency (EQE) is the ratio of the number of charge carriers collected by the solar cell to the number of photons of a given energy shining on the solar cell from outside (incident photons).

- Internal Quantum Efficiency (IQE) is the ratio of the number of charge carriers collected by the solar cell to the number of photons of a given energy that shine on the solar cell from outside and are absorbed by the cell [13].

II.2.5. Losses in Solar Cells

The conversion efficiency of a real solar cell is generally lower than that of an ideal solar cell due to the various loss factors, some of these are avoidable but others are intrinsic to the system [2], The main reasons for these losses are described below.

II.2.5.1. Optical losses

A solar cell comprises numerous layers, some of which can contribute to parasitic photon absorption or absorption that does not contribute in the formation of the electron/hole pair. Hence during the fabrication of solar cells, it is important to evaluate the absorbance of the front-layers.

In addition, reflection may contribute in optical losses. In modern silicon solar cells this effect is avoided using anti-reflective coatings.

II.2.5.2. Resistive losses (shunt and series resistance)

The Shockley equation in real solar cells is influenced by shunt (R_{SH}) and series (R_S) resistances, as these allow power dissipation. Their effect on the shapes of the *J-V* curves, is shown in **Figure II.6**. The series resistance is commonly associated with thick absorbing layers, low doping levels and low conductivity of the front transparent contact, whereas the shunt resistance may occur in case of layers with pin-holes and weak diode regions.

The resistances values may be determined by measuring the inverse of the slope close to the V_{OC} and J_{SC} for R_S and R_{SH} respectively. In order to have the smallest influence on the solar cell, R_S should approach 0, whereas R_{SH} should tend toward infinity.

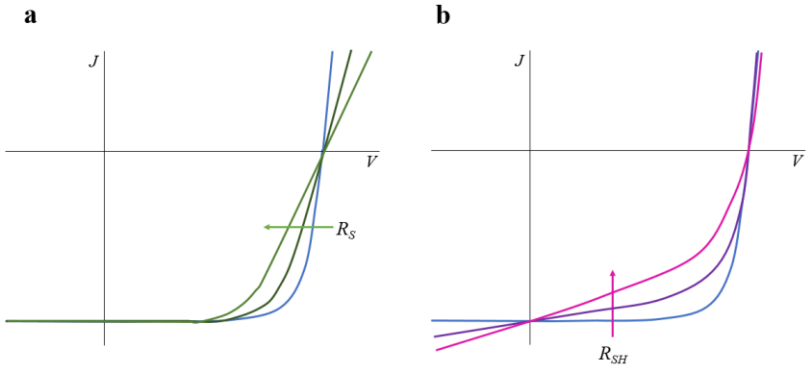

Figure II.6. J-V curves showing the effect of series (a) and shunt (b) resistances on the curve.

II.2.5.3. Recombination losses

Electron/hole pair generated by photon absorption, may be subjected to recombination in the bulk, on the surface or in the depletion region. Recombination losses affect both J_{SC} and V_{OC} and are caused by native defects, impurities, or dangling bonds.

Bulk recombination effects may occur in three different ways: radiative, nonradiative and Auger recombination.

II.2.5.4. Metal-semiconductor interface losses

While for Ohmic contacts electrons and holes are free to move in and out of a semiconductor with minimal energy losses, in Schottky junctions (rectifying contacts) the potential barrier causes a reduction in the carrier flow. Since in a solar cell the Schottky junction behaves similarly to a second diode, a 'roll-over' at forward bias may be recorded in a *J-V* curve (Figure II.7), which may affect the V_{OC} of the solar cell [11].

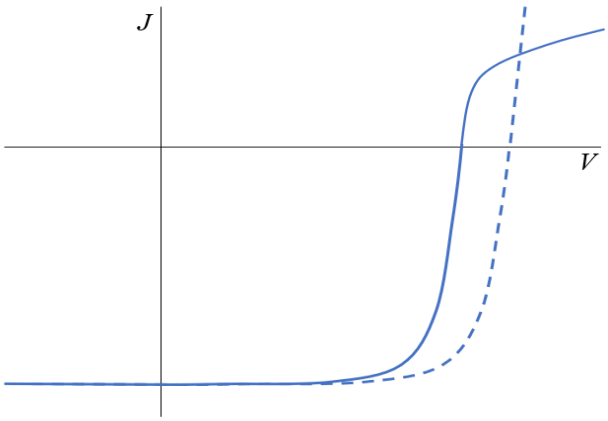

Figure II.7. 'Roll-over' effect caused by a back contact junction diode.

II.2.6. Solar cell types

According to M. A. Green's classification there are three major classes of solar cells (first, second and third generation). This classification is based on the nature of the material, the maximum efficiency reachable, and the cost of each type. There are a lot of researches into all these types but the first-generation technologies are dominant in the commercial production [2].

II.2.6.1. First Generation

The traditional Solar cells made of mono crystalline Si, GaAs, polycrystalline Si, and etc. come under this category. More than 80% of installed solar panels today are first generation. Huge fluctuation in raw material cost and the cell efficiency nearing its theoretical maximum limit [14]. Made today's researchers concentrate on the other two generations.

II.2.6.2. Second Generation

The high production costs of the first generation solar cells have caused researchers to focus on the second generation solar cells. These second generation cells use photo voltaic materials which are easy to grow and and less pure. A-Si (amorphous silicon), CdTe (cadmium telluride), CIGS (copper indium gallium arsenide) are some of these.

II.2.6.3. Third Generation

The solar cells which are able to achieve the efficiency greater than the Shockley-Queisser efficiency limit are categorized as third generation solar cells. Quantum dots, multi junction tandem cells, solar thermal, dye synthesized solar cells, organic photovoltaic etc. technologies can be classified as third generation.

Most of the third generation solar cell technologies are not yet commercially viable. But extended research may cause a substantial increase in the efficiency and lowering of the production costs [15].

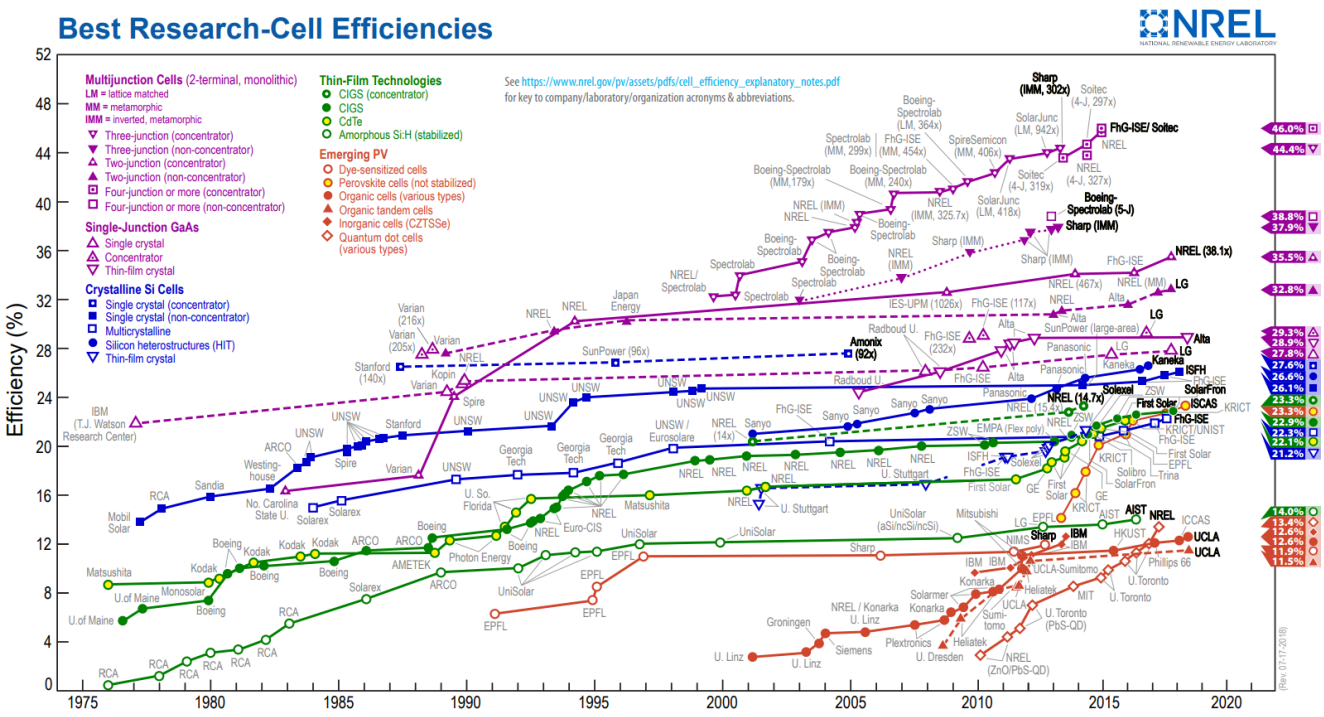

Figure II.8. Schematic of best achievable efficiencies in different types of solar cells [4].

References

[1] C. FRISK, *Modeling and electrical characterization of Cu(In,Ga)Se2 and Cu2ZnSnS4 solar cells, Uppsala University,* 2017.

[2] A. Ghania, *STUDY OF SILICON SOLAR CELLS PERFORMANCES USING THE IMPURITY PHOTOVOLTAIC EFFECT, DOCTORAT thesis, Université Ferhat Abbas–Setif,* 2012.

[3] B. Padmanabhan, *MODELING OF SOLAR CELLS, Master thesis, ARIZONA STATE UNIVERSITY,* 2008.

[4] A. HAMACHE, *Study of the type inversion of the semiconductor in irradiated solar cells, doctorate thesis, Mohamed Khider University,* 2018.

[5] G. N. Tiwari, Solar Energy: Fundamentals, Design, Modelling and Applications, Narosa, Publishing House, New Delhi, India, 2004.

[6] M. A. Green, Solar cells, Operating Principles Technology, and Systems, Prentice-Hall, 1982.

[7] P. .. Nwofe, *Deposition and Characterisation of SnS Thin Films for Application inPhotovoltaic Solar Cell Devices, PhD thesis, University of Northumbria at Newcastle,* 2013.

[8] Adolf Goetzberger, Volker U. Hoffmann, H.K.V. Lotsch, Photovoltaic solar energy generation, Springer Verlag Berlin, 2005.

[9] J. V. Holm, *Nanowire Growth for Photovoltaics, PhD thesis, University of Copenhagen,* 2013.

[10] G. ALTAMURA, *Development of CZTSSe thin Films based solar cells, PhD thesis, University of Grenoble,* 2014.

[11] S. Mariotti, *Hybrid and inorganic plumbo-halide perovskites for solar cells, Doctorate thesis, university of liverpool,* 2019.

[12] M. A. Green, «The Path to 25% Silicon Solar Cell Efficiency: History of Silicon Cell Evolution,» *Progress in Photovoltaics,* vol. 17, pp. 183-189, 2009.

[13] Augustin McEvoy, Tom Markvart, Luis Castañer, Practical Handbook of Photovoltaics Fundamentals and Applications, 2012.

[14] WILLIAM SHOCKLEY, HANS J. QUEISSER, «Detailed Balance Limit of Efficiency of p-n Junction Solar Cells,» *JOURNAL OF APPLIED PHYSICS,* vol. 32, n° %13, pp. 510-519, 1961.

[15] M. Morusu, *Investigation of CZTSe Solar Cell with ZnS, ZnSe and In2S3 as Buffer Layers, master thesis, University of Toledo,* 2012.

Practical part

Chapter III : ZnS elaboration

III.1. Introduction :

This chapter is dedicated to the description of the different experimental techniques used in this work. On a glass substrate, we deposit ZnS thin films form aqueous solution alcohol containing zinc acetate dihydrate ($ZnC_4H_6O_4.2H_2O$) and thiourea ($CS(NH_2)_2$) in a volume of methanol CH_3OH as a solvent on heated glass substrates using ultrasonic spray process.

III.2. Choice and preparation of substrate

In our work, the glass substrates used are equidistant (**Figure III.1**) that are sterilized by solvent solutions (distilled water, acetone, and ethanol) and dried with Joseph paper in the following steps:

Figure III.1. Isometric glass substrates and diamond pen.

- The glass substrates have cut into equal dimensional substrates by pen of diamond point (Figure II.9),
- Soak the substrates in acetone to remove grease and fats,
- The substrates are immersed in distilled water to remove traces of acetone,
- Soak the substrates in ethanol to remove the organic matter. The substrates are again immersed in distilled water to remove traces ethanol,
- The glass slides ultrasonically cleaned in each for about 5 min,
- Drying the substrates using Joseph paper, so as not to leave any traces or impurities.

III.3. Preparation of precursor solutions

There are several precursors to obtain thin films of Zinc Sulfide, but in our work, we have chosen zinc acetate dihydrate and thiourea dissolved in aqueous alcohol solution; with molarity **C** equal to 0.1 mol/l. By following these steps:

- Measure a mass of zinc acetate dihydrate m = C.M.V using a balance (the molar mass $M_{ZnC4H6O4}$ = 183.48 and $M_{CS(NH2)2}$ = 76.12);
- The previous mass was dissolved in an aqueous alcohol solution by volume V = 60ml;
- The solution was stirred with ultrasonic bath cleaners for about five minutes;

III.4. Ultrasonic spray pyrolysis's equipment

We have developed zinc sulphide thin films using ultrasonic spray pyrolysis technique (**Figure III.2**), at laboratory of semiconductors of Annaba University.

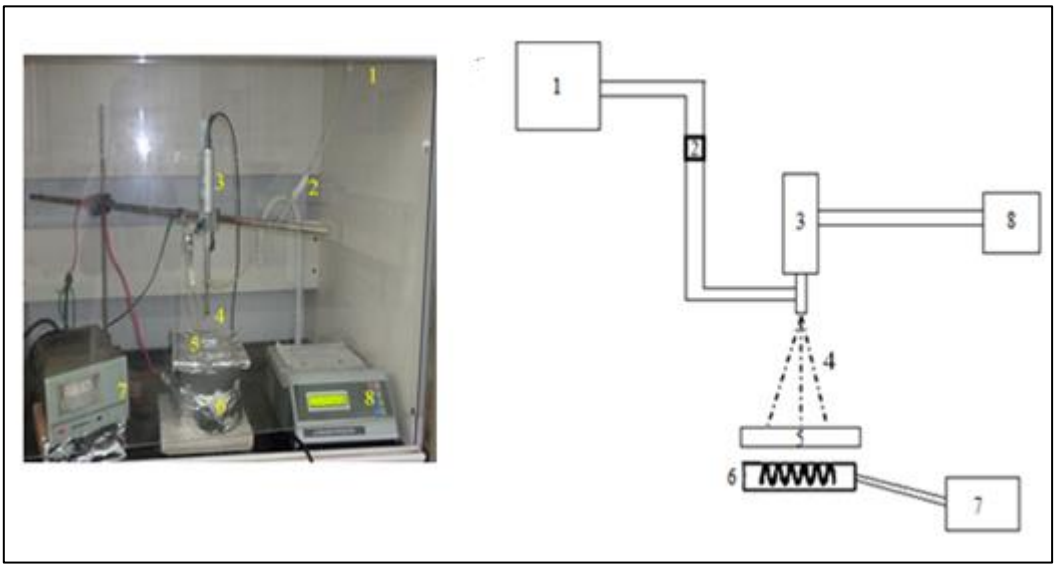

Figure III.2. Complete experimental devices of the ultrasonic spray pyrolysis technique.

The main elements of the experimental set up of the spray pyrolysis system are:

1. Ultrasonic generator (40 KHz): allows decomposing the solution at the atomizer to very fine droplets (Ø ~40 µm);
2. Atomizer: the atomizer is placed on a support height adjustable to control the nozzle spray distance;
3. Substrate heater: it is substrate holder (Ø =25 cm) heated by joule effect.

III.5. Preparation of thin films

After preparing the substrates and solutions, all samples are preparation through the following steps:

- The prepared solution with the molarity 0. 1M by using methanol solvent is placed in a solution holder to be sprayed in the form of very thin drops, using ultrasonic generator, that

precipitate over the glass substrate. Before deposition, the substrates were kept at ambient temperature to avoid thermal shock.

- The substrates were heated to (300, 400 and 500 °C) temperature for each film.
- The nozzle was kept at a distance of 5 cm from the substrate during deposition.
- The spray rate was maintained at 60 ml/h using an ultrasonic generator (40 kHz).
- The spraying time (35 min) was maintained each time. When aerosol droplets came close to the substrates, the compounds reacted to become a new chemical compound ZnS.

Table III.1: Process parameters for the spray deposition of ZnS thin films.

Precursor / molarity	**Zinc acetate ($ZnC_4H_6O_4$) 0.1 mol/l**		**Thiourea ($SC(NH_2)_2$) 0.1 mol/l**
Deposition time (min)	35		
Volume (ml)	60		
Nozzle-substrate distance (cm)	5 cm		
Pression	Atmosphérique (1 atm)		
Substrate temperature (°C)	300	400	500

Chapter IV : Results and discussion

IV.1. Introduction

As commonly known, that the ZnS thin films properties are significant effected by technique of elaboration and deposition parameters. In the case of ultrasonic spray pyrolysis, the main parameter which is widely influenced on ZnS thin films properties is substrate temperature which controls the spices energy and motion onto substrate surface.

The purpose of this chapter is to present and interpret the experimental results of this work which aims the elaboration and characterization of zinc sulphide thin films deposited on glass substrates by ultrasonic spray pyrolysis technique at different substrate temperatures (300, 400 and 500 °C).

IV.2. Experimental details

ZnS thin films were prepared by spraying a solution contains a 0.1 mol/l of zinc acetate ($ZnC_4H_6O_4.2H_2O$) and thiourea ($CS(NH_2)_2$) in a volume of methanol CH_3OH as a solvent on heated glass substrates using ultrasonic spray process. The elaborated films were characterized in order to study their properties. The films structure was analyzed by X-ray diffraction using XPERT-PRO diffract meter. The Morphological properties were studied using both of SEM and EDS methods. The optical transmittance spectra in UV–Visible rang was achieved using Perkin Elmer spectrophotometer. And solar cells using those films were studied.

IV.3. Structural properties

IV.3.1 XRD analysis

The X-rays diffraction is carried out to study the crystalline quality of the ZnS thin films elaborated at various substrate temperatures. **Figure IV.1** shows the XRD pattern of the samples. In all the films, the basic peaks were (111), (200) and (220) planes were assigned to the 28.52°, 33.07° and 47.52°, respectively, according to the diffraction profiles (JCPDS Card No. 05-0566).

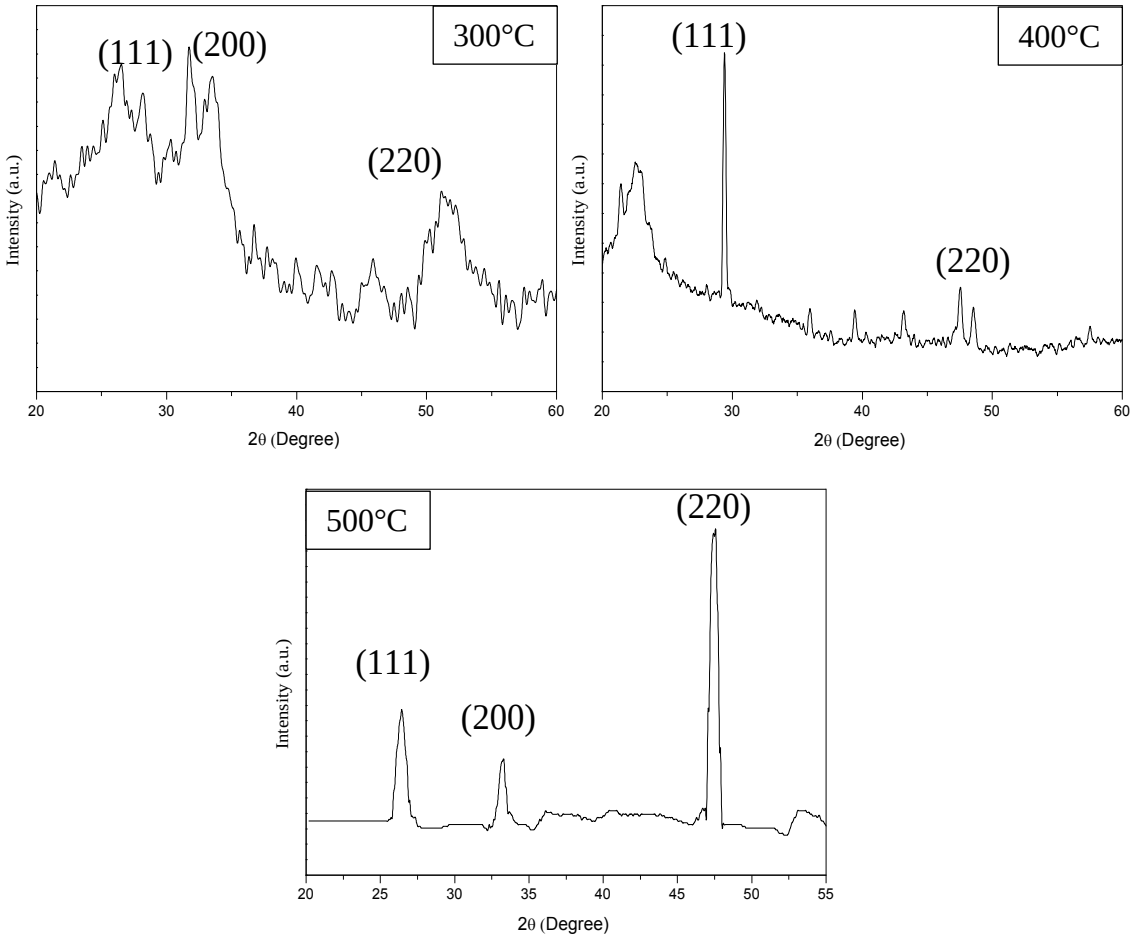

Figure IV.1. XRD patterns of zinc sulfide as function of substrate temperature.

It can be seen that the formation of ZnS crystallites in the films elaborated at low deposition temperature (Ts = 300°C).

The XRD patterns revealed the formation of pure ZnS thin films for all the deposited samples with different substrate temperatures. For Ts = 300 °C, a wide peak in the form of a bump was observed, indicating that an amorphous phase is present in the prepared ZnS film. The ZnS crystal structure improves at Ts > 300 ° C. This crystallinity improvement is due to the temperature rise, which contributes to the ZnS pure phase growth. This can be explained by the fact that kinetic energy is directly proportional to the applied temperature.

Basically, with the increase of the temperature, the vibration/collision of the molecules increases, and this also applies to the kinetic energy. Thus, some of the absorbed energy is stored within the particles, while some of the energy increases the motion of the particles, leading to the formation of the Zn-S boundaries from which the ZnS is obtained.

Our findings show that increasing the temperature improved the crystallization of the ZnS films.

IV.3.2. Crystallite size

The crystallite size (D) represent the crystalline quality of the ZnS films. It was calculated using the classical Scherrer formula [1, 2].

$$D = k.\lambda/\beta \cos\theta \qquad \text{(IV.1)}$$

Where λ is the X-ray wavelength of radiation, θ is the Bragg angle, β is FWHM calculated in radians. For the CuKa line, the shape factor k equal to 0.9.

Figure. III.2 represents the variation of crystallite size with the substrate temperature. The crystallite size is calculated from the most intense diffraction peak for each sample.

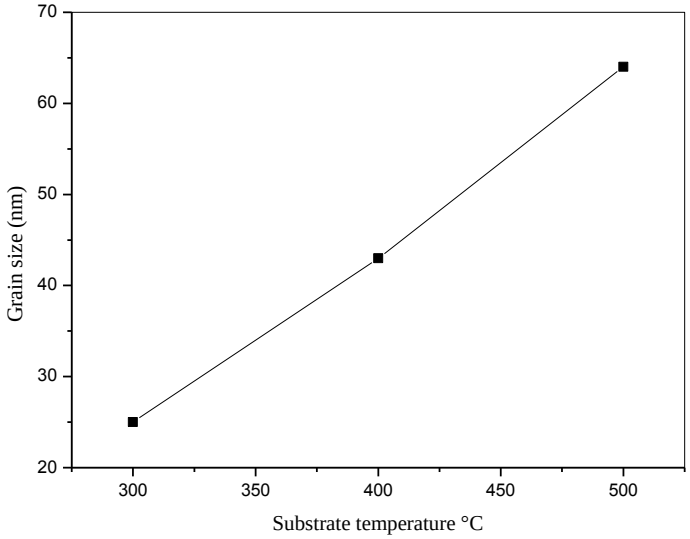

Figure IV.2. crystallite size of ZnS thin films as a function of substrate temperature.

It can be remarked that crystallite size increases with increasing the substrate temperature from 25 nm for Ts = 300 °C to 64 nm for Ts = 500 °C. Therefore, the prepared ZnS films can be viewed as nanocrystalline or nano-structured films. It is also noted that the films produced at high temperatures contain larger sized crystallites, which leads to the reduction of the strain as well as the stresses in the crystal lattice of the films and, consequently, to the improvement of the crystallinity of the ZnS structure, as has been well confirmed by the XRD spectra.

IV.3.3. Microstrain and dislocation

Microstrain (ε) of ZnS films was deduced by using the following equation [3, 4]:

$$\boldsymbol{\varepsilon = \frac{\beta \cos\theta}{4}} \qquad \text{(IV.2)}$$

The variation of ε as a function of substrate temperature is given in figure IV.3.

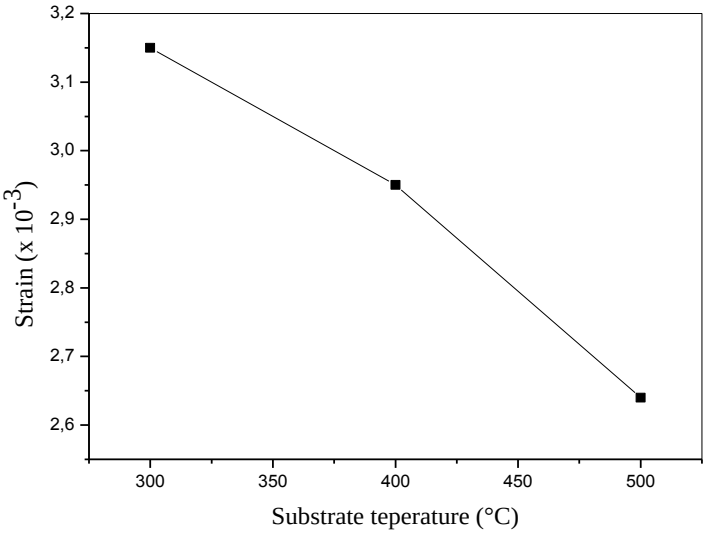

Figure IV.3. Microstrain of ZnS thin films as a function of substrate temperature.

The increase of substrate temperature more than 300 °C engender the increase of crystallite size. The rise of crystallite size results of the decrease of lattice strain ε due to reduction in defect density inside the films, which involves a network relaxation [5, 6]. In this case, the crystalline state of the films has been improved and the growth mode changed to island growth with increasing the substrate temperature due to decrease total surface energy which impose the sprayed material species to create a small island perpendicular on substrate surface.

A dislocation is a crystallographic fault or imperfection that occurs inside a crystal structure. Several material properties are affected by the presence of dislocations [7]. The density of dislocations was calculated employing the formula [8, 9]:

$$\delta = \frac{1}{D^2} \qquad \text{(IV.3)}$$

The variation of the dislocation density is shown in figure IV.4.

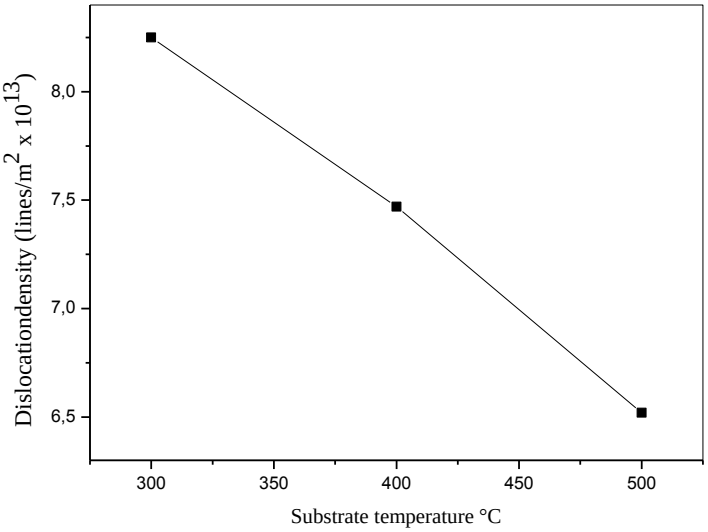

Figure IV.4. Dislocation density of ZnS thin films versus the substrate temperature.

As grain size grows, δ and ε decrease, indicating better crystallinity. Same findings are published by Hasanzadeh [10, 11].

IV.4. Morphological properties and chemical composition

IV.4.1. Morphological properties

SEM micrographs of ZnS films deposited at different substrate temperatures are shown in figure IV.5.

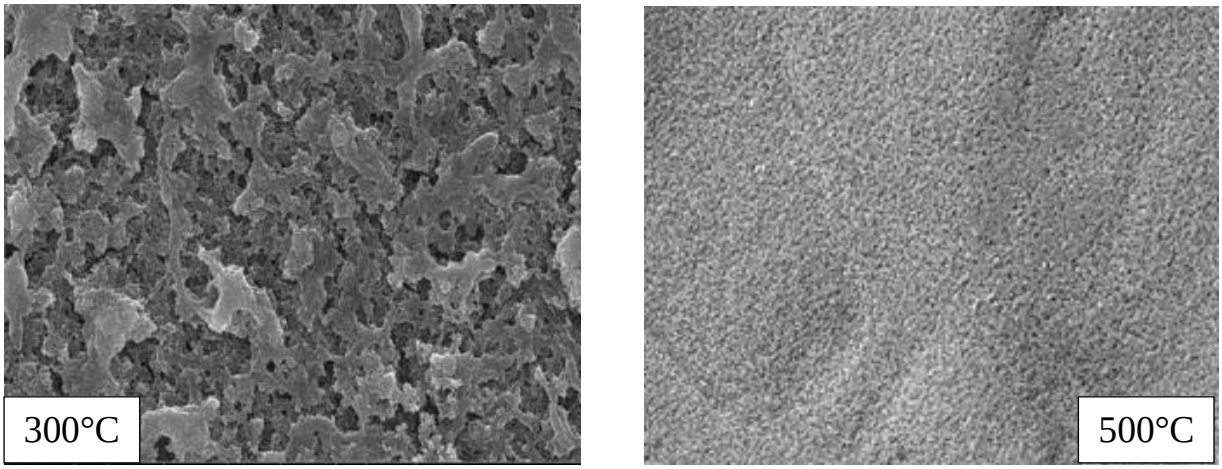

Figure IV.5. SEM images of ZnS films deposited at different substrate temperatures.

SEM micrographs showed that the film's surface deposited at T_S = 300 °C has an inhomogeneous and discontinuous structure full of cracks with a rough morphology. This indicates that an amorphous phase is present in the deposited ZnS film. For T_S = 500 °C, the surface topography of the ZnS film is devoid of cracks, dense and smooth with an arbitrary

distribution of the bubbles due to the blowing up of the surface caused by the exo-diffusion of sulfur [12].

IV.4.2. Compositional analysis

Energy Dispersive X-ray Spectrometer (EDS) was used to study the compositional analysis of ZnS films. **Figure IV.6** shows the EDS spectrum of the surface film. The elemental analysis shows the presence of Zinc (Zn) and sulfur (S) along with some other elements. In the spectra, a carbon peak is observed due to the substrate holder and an oxygen peak might be due to the partial oxidation of the film. Presence of Si and Sn results from the substrate. The relative average atomic percentage ratio of Zn:S is nearly 1:1 for the films, indicating the formation of a film with stoichiometric composition.

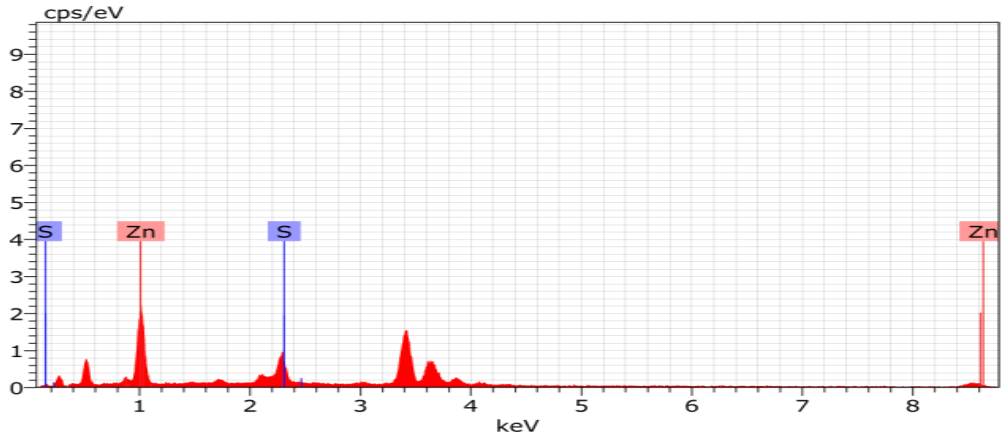

Figure IV.6. The EDS spectra of ZnS film obtained at 500 °C.

IV.5. Optical properties

Transmitting spectrum of ZnS thin films were observed in the UV-visible ranges (350-800) nm and they are given in Figure IV.7.

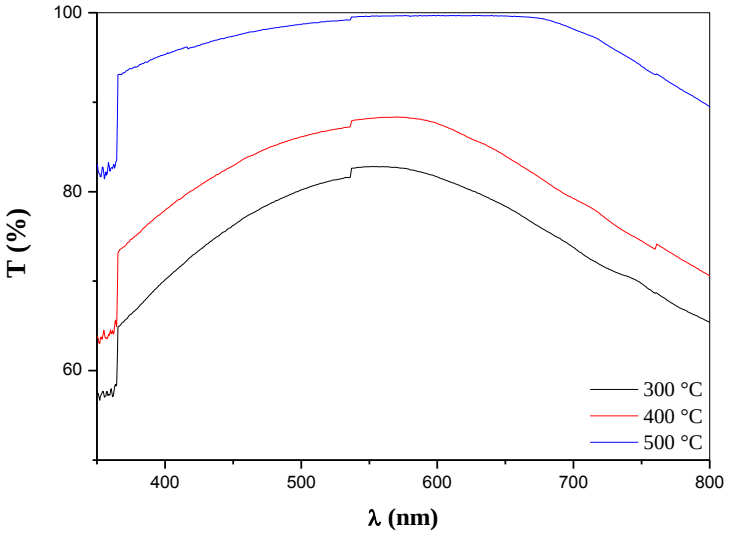

Figure IV.7. Transmittance spectra of ZnS thin films.

Considering that these spectra were obtained taking the substrate as reference signal I_0, typical tails in the absorption edge of the layers can be observed, which is related to the formation of located states in the band gap of the layers deposited by spray method. Moreover, the pure crystalline quality of the nanometric thin layers does not result in sharp absorption edges at the band gap values of ZnS layers.

Nevertheless, a shift towards the small wavelength region with a lowering of ZnS thickness is observed, which can be explained by the quantum confinement effect, and in combination with wide band gap of ZnS results in increasing of the transmittance in the blue spectral range. Furthermore, the increase in transmittance is in good agreement with the decrease of the thickness (not shown).

IV.6. Solar cell assembly and characteristics modelization

Figure IV.8 shows the schematic of ZnS/CZTSe based solar cell studied in this work.

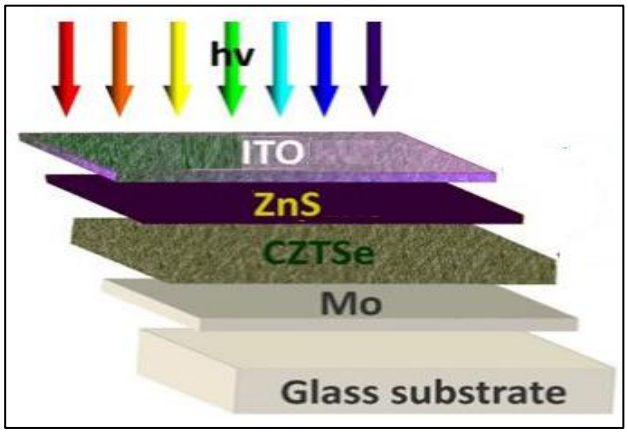

Figure IV.8. Schematic structure of CZTSe solar cells with a cross section of the device.

The distribution of the illuminated J-V curves of the best solar cell of this work as well as dark J-V measurement are depicted in Figure III.9 (A). The external quantum efficiency (EQE) of the selected devices is depicted in Figure III.9 (B).

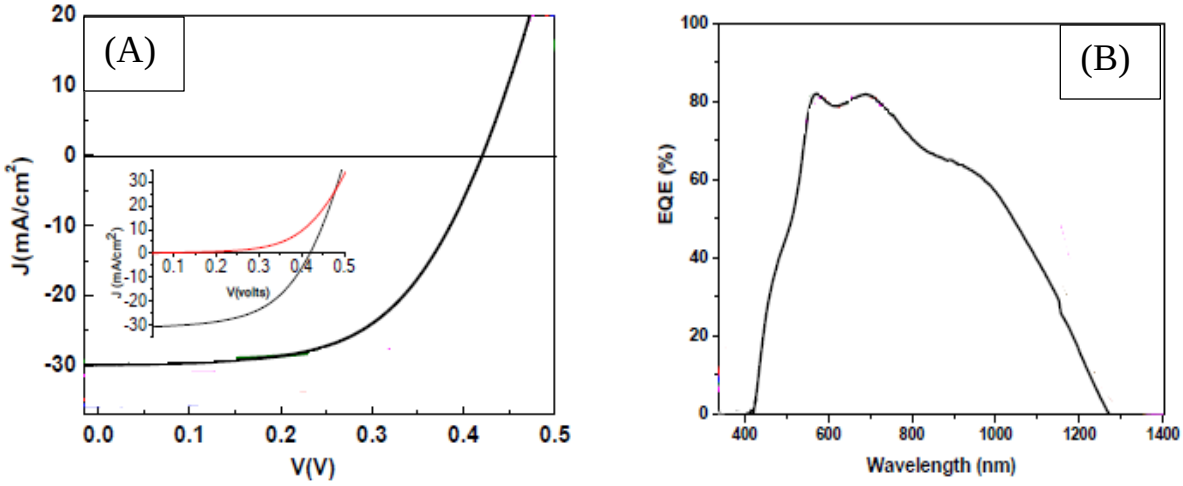

Figure IV.9. (A) illuminated J-V curves of ZnS based thin film solar cells and in the inset the comparison between the dark and illuminated devices of the reference ZnS/CZTSe based solar cells. (B) Simulated external quantum efficiency (EQE) data of the solar cells.

From **Figure IV.9 (A)** we can observe, a slight increase in the current density value where cross-over occurs was observed for ZnS buffer layer, deep acceptor-like traps could modify the conduction band alignment, increasing the spike that acts as a barrier for photogenerated electrons like a second diode.

According to the **Figure IV.9 (B)** we can notice that the EQE value is above 60 % in the range of 300 – 1000 nm, indicating that most of the photo-generated electron-hole pairs are able to reach the space charge region, and contribute to the charge separation in the cells. These results are in agreement with the optical transmittance spectra of the buffer layer (**Figure IV.7**).

References

[1] Hadi, E.H., Sabur, D.A., Chiad, S.S., Habubi, N.F., Abass, K.H., Journal of Green Engineering, 10 (10), 8390-8400 (2020).

[2] Hussin, H.A., Al-Hasnawy, R.S., Jasim, R.I., Habubi, N.F., Chiad, S.S., Journal of Green Engineering, 10(9) 7018-7028 (2020).

[3] Latif, D.M.A., Chiad, S.S., Erhayief, M.S., Abass, K.H., Habubi, N.F., Hussin, H.A., Journal of Physics, Conference Series 1003(1) 012108 (2018).
https://doi.org/10.1088/1742-6596/1003/1/012108

[4] Othman, M.S., Mishjil, K.A., Rashid, H.G., Chiad, S.S., Habubi, N.F., Al-Baidhany, Journal of Materials Science: Materials in Electronics, 31(11), 9037-9043 (2020). https://doi.org/10.1007/s10854-020-03437-0

[5] MalleKrunks, EnnMellikov,Thin Solid Films 270 (1995) 33-36**.**

[6] P.R.Benger, K.Chang, P.Bhattacharya, J.Sing, K.K.Bajaj, Appl. Phys. Lett.53 (1988) 684–686.

[7] G.K. Williamson, R.E. Smallman, Philosophical Magazine, 1, 34-45 (1956). https://doi.org/10.1080/14786435608238074

[8] Ali, R.S., Mohammed, S.A.A., Mohammed, A.H., IOP Conference Series: Materials Science and Engineering, , 928(7), 072154 (2020). https://doi:10.1088/1757-899X/928/7/072154

[9]Sulaiman, H.T., Ali, R.S., Khoudhair, M.J., Mohammed, S.A.A. Neuro Quantologythis, 18(1), 99–10 (2020). https://doi:10.14704/nq.2020.18.1. NQ20113.

[10] J. Hasanzadeh, A. Taherkhani and M. Ghorbani, Chinese journal of physics, 51 (3), 540-550(2013).

[11] A.S. Hasan, N. B. Hasan, A. J. Hayder, The first scientific conference for college of science, University of Karbala, pp.18-25(2013).

[12] B. Shin, O. Gunawan, Y. Zhu, N. A. Bojarczuk, S. Jay Chey and S. Guha,Thin film solar cell with 8.4% power conversion efficiency using an earth-abundant Cu2ZnSnS4 absorber, Progress in Photovoltaics 21 (2013) 72-76.

General Conclusion

In this study ZnS thin films were prepared by ultrasonic spray pyrolysis technique at different substrate temperatures (300, 400 and 500 °C), The elaborated films were characterized in order to study their properties. The film's structure and chemical composition was analyzed by X-ray diffraction using XPERT-PRO diffract meter. The Morphological properties were studied using both of SEM and EDS methods. The optical transmittance spectra in UV–Visible rang was achieved using Perkin Elmer spectrophotometer. And solar cells using those films were studied. The most important results obtained can be summarized as follows:

- The ZnS film exhibits the reflection planes (111), (200) and (220) that were assigned to the 28.52°, 33.07° and 47.52°, respectively.
- Increasing the substrate temperature improved the crystallization of the ZnS films.
- The crystallite size increases with increasing the substrate temperature from 25 nm for T_S = 300 °C to 64 nm for T_S = 500 °C, which leads to the reduction of the strain as well as the stresses in the crystal lattice of the films.
- The rise of crystallite size results of the decrease of lattice strain ε and Dislocation density due to reduction in defect density inside the films.
- SEM micrographs of ZnS films shows that the film's surface deposited at T_S = 300°C has an inhomogeneous and discontinuous structure full of cracks with a rough morphology. Thus, for T_S = 500 °C, the surface topography of the ZnS film is devoid of cracks, dense and smooth.
- Energy Dispersive X-ray Spectrometer elemental analysis shows that the films aren't pure as we see the presence of Zn, S, C, O, Si and Sn but the relative average atomic percentage ratio of Zn:S is nearly 1:1 for the films, indicating the formation of a film with stoichiometric composition
- The increasing of the transmittance of the films in the blue spectral range and the increase in transmittance is in good agreement with the decrease of the thickness.
- ZnS films in solar cells shows promising results, the J-V curves of the best solar cell of this work was distributed besides the external quantum efficiency of the selectesd devices.
- the EQE value is above 60 % in the range of 300 – 1000 nm, indicating that most of the photo-generated electron-hole pairs are able to reach the space charge region, and contribute to the charge separation in the cells, with the highest EQE noted in this study is around 84% for a wavelength around 550 nm.